(2)

GL-TR-90-0178
ENVIRONMENTAL RESEARCH PAPERS, NO. 1065

Data Report for the 1988 Ontario-New York-New England Seismic Refraction Experiment: Small-Aperture Array

JAMES C. BATTIS

6 July 1990

Approved for public release; distribution unlimited.

EARTH SCIENCES DIVISION PROJECT 7600
GEOPHYSICS LABORATORY
HANSCOM AFB, MA 01731-5000

"This technical report has been reviewed and is approved for publication"

JAMES F. LEWKOWICZ, Chief
Solid Earth Geophysics Branch

DONALD H. ECKHARDT, Director
Earth Sciences Division

This report has been reviewed by the ESD Public Affairs Office (PA) and is releasable to the National Technical Information Service (NTIS).

Qualified requestors may obtain additional copies from the Defense Technical Information Center. All others should apply to the National Technical Information Service.

If your address has changed, or if you wish to be removed from the mailing list, or if the addressee is no longer employed by your organization, please notify GL/IMA, Hanscom AFB, MA 01731. This will assist us in maintaining a current mailing list.

REPORT DOCUMENTATION PAGE

Form Approved
OMB No 0704 0188

1. AGENCY USE ONLY (Leave blank)	2. REPORT DATE 6 July 1990	3. REPORT TYPE AND DATES COVERED Scientific, Final (1 OCT 88 to 30 SEP 89)
4. TITLE AND SUBTITLE Data Report for the 1988 Ontario-New York-New England Seismic Refraction Experiment: Small-Aperture Array		5. FUNDING NUMBERS PE62101F PR7600 TA09 WU09
6. AUTHOR(S) James C. Battis		
7. PERFORMING ORGANIZATION NAME(S) AND ADDRESS(ES) Geophysics Laboratory (LWH) Hanscom AFB, MA 01731-5000		8. PERFORMING ORGANIZATION REPORT NUMBER GL-TR-90-0178 ERP, No. 1065
9. SPONSORING MONITORING AGENCY NAME(S) AND ADDRESS(ES)		10. SPONSORING/MONITORING AGENCY REPORT NUMBER
11. SUPPLEMENTARY NOTES		
12a. DISTRIBUTION AVAILABILITY STATEMENT Approved for public release, distribution unlimited.		12b. DISTRIBUTION CODE

13. ABSTRACT (Maximum 200 words)

During September 1988 the Solid Earth Geophysics Branch of the Geophysics Laboratory Earth Sciences Division, GL/LWH, supported a major crustal refraction and wide-angle reflection survey transecting New England, New York and continuing into Ontario, Canada. This experiment, the Ontario-New York-New England Seismic Refraction Experiment, was conducted jointly between the Geophysics Laboratory (GL), the US Geologic Survey (USGS), and the Geological Survey of Canada (GSC). The purpose of this program was to better understand the geologic structure and wave propagation characteristics across the northern Appalachians of New England and into the Grenville province to the west. Data collection along the main transect was largely carried out by field teams from the USGS and the GSC. In addition, GL conducted two field programs during the experiment. The main effort was the operation of a series of three-component seismic refraction lines across upstate New York and Vermont. GL/LWH also operated a small-aperture array near North Haverhill, New Hampshire. This report provides technical background on the data collected by that array.

14. SUBJECT TERMS Key words: Seismology, Crustal structure, Seismic refraction, Seismic array.			15. NUMBER OF PAGES 58
			16. PRICE CODE
17. SECURITY CLASSIFICATION OF REPORT Unclassified	18. SECURITY CLASSIFICATION OF THIS PAGE Unclassified	19. SECURITY CLASSIFICATION OF ABSTRACT Unclassified	20. LIMITATION OF ABSTRACT S.A.R.

Acknowledgements

The author expresses his appreciation to Mr. Joseph Blaney and Mr. Christopher Center of Weston Observatory of Boston College, Capt. Lloyd Rainey and Sgt. Joseph Craig of the Geophysics Laboratory (GL) and Dr. Anton Dainty, a National Research Council Research Associate at GL, for assisting in the array setup and operation during the field experiment and the subsequent data reduction process. I would also express my appreciation to the community of North Haverhill, New Hampshire for allowing access to the Dean Memorial Airport site and, in particular, Mr. James Fortier, the airport manager, Mr. Roland McKean, the groundskeeper, and Mr. David Hatch, leaseholder on the airport property, without whose cooperation this effort would have been impossible.

Contents

Illustrations

Tables

Data Report for the 1988 Ontario-New York-New England Seismic Refraction Experiment: Small-Aperture Array

1. INTRODUCTION

During September 1988 the Solid Earth Geophysics Branch of the Geophysics Laboratory Earth Sciences Division supported a major crustal refraction and wide-angle reflection survey transecting New England, New York and continuing into Ontario, Canada. This experiment, the Ontario-New York-New England Seismic Refraction Experiment, was conducted jointly between the Geophysics Laboratory (GL), the US Geologic Survey (USGS), and the Geological Survey of Canada (GSC). The purpose of this program was to better understand the geologic structure and wave propagation characteristics across the northern Appalachians of New England and into the Grenville province to the west. The area of the study for this experiment is shown in Figure 1.

Data collection along the main transect was largely carried out by field teams from the USGS and the GSC [*Luetgert* et al., 1990]. GL conducted two field programs during the experiment. The main effort was the operation of a series of three-component seismic refraction lines across upstate New York and Vermont [*Mangino and Cipar*, 1990] and the second was the operation of a small-aperture array in northern New Hampshire. In addition, several universities, and at least one private company, conducted "add-on" experiments. These organizations included the State University of New York at Binghamton, Boston College, Lamont Doherty Geological Observatory, Yale University, Massachusetts Institute of Technology, and Rondout Associates.

The GL small-aperture array was a 16-element seismic array located at North Haverhill, New Hampshire (Figure 1). This report is a compilation of basic information on this array, including configuration and operation information, and displays of the data collected during the experiment. Interpretation of these data will be published separately. All data discussed in this report are available by contacting the Earth Sciences Division of the Geophysics Laboratory at:

GL/LWH
Hanscom AFB, MA 01731-5000
Telephone 617-377-3222

Received for publication 5 July 1990

2. THE NORTH HAVERHILL SMALL-APERTURE ARRAY

2.1 The Array Location and Geology

The GL seismic array was located on the property of a small municipal airport in the town of North Haverhill, New Hampshire. Installation began on 6 September and the array was operational through 30 September. The latitude and longitude of the array, referenced to the vertex of the arms, was measured to be 44.079°N and 72.009°W at an elevation of 177 meters above mean sea level (Figure 2). Geophysically, the site is of interest as it lies near the contact line between the ancient North American and European or African plates. Shots to the east of the site are basically propagating through the alien crust while those from the west travel in the proto-North American plate, as defined by the limits of Grenville formations.

This array was sited within the Connecticut River Valley and just west of the White Mountain plutons. It lies between the Foster Hill sole fault on the east and the Ammonoosuc fault on the west, both of which trend north-northeast in the area of the array (*Moench*, 1989). The Ammonoosuc fault is taken to be the western boundary of the Bronson Hill anticlinorium, an island arc complex associated with the overthrusting of the oceanic plates during the closing of the proto-Atlantic ocean. This event occurred about 440 million years ago, during the middle Ordovician. The site is at the northern end of the Piermont Allochthon which appears to have been transported to its present location during the Acadian orogeny and before the emplacement of the Devonian New Hampshire Plutonic Series. The array was located just outside of the mapped southern boundary of the French Pond pluton from this series. Underlaying the site and extending well to the south is a turbidite sequence of interbedded metasandstones and phyllites, part of the allochthon. Both the allochthon and the plutonic intrusions are typical of continental convergence zones as hypothesized for the Acadian orogeny (*Dewey*, 1977).

2.2 Shallow Seismic Velocity Structure

During the operation of the array, a seismic survey of the site was conducted to estimate the shallow velocity structure. This survey was made by generating several hammer blows on the ground surface at each sensor location and recording the responses of the remaining sensors of the array. The sensor at which the hammer blows were being generated was replaced by an accelerometer attached to the hammer. The output of this accelerometer marked the origin time for each hammer blow. Processing of the hammer blow data consisted of aligning and stacking the responses for each channel from all the hammer blows generated at a given sensor, correcting for instrument response and bandpass filtering the resulting traces over the range of 10.0 to 34.3 Hz. The parameters of the bandpass, selected on the basis of the seismic spectra from a wide range of distances of the hammer blow pulse generated at this site, represent the band having sufficient signal to noise ratio to provide high quality surface wave data. The resulting traces provided two types of data for analysis. As expected from hammer blow type data, weak P-wave arrivals were recorded preceding a dominant Rayleigh wave.

Travel times from the P-wave arrivals were used for refraction modeling. Although the refraction data were considered to be of low quality, they suggested a two layer model with an 11 m thick surficial layer having a P-wave velocity of 756 m/sec overlying a half-space with a P-wave velocity of about 1943 m/sec.

More extensive analysis was performed with the Rayleigh wave component of the traces. Using software developed by Herrmann (1989), group velocity dispersion curves were estimated for each arm of the array from the hammer blow data and velocity models were generated by inversion of these curves. These dispersion curves and the fit curves are shown in Figure 3. The derived velocity structures for each arm of the array are given in Table 1 and plotted in Figures 4a and 4b. It should be noted that inversion of the Rayleigh wave group velocity provided the shear velocity model. The compressional velocities were generated from the shear velocity model using a Poisson's ratio of 0.25.

Although the refraction data obtained from the hammer blows was considered of low quality and showed a high level of scatter, it does, in a broad sense, support the surface wave inversion structure in that both models indicate a major velocity discontinuity at approximately 10 to 15 m depth although the refraction-derived velocity below this discontinuity appears to be substantially higher than that estimated by group velocity inversion, approximately 1950 m/sec.

It is noted that sufficient uncertainty exists in the observed dispersion curves and for the estimated shear velocity models that either of the two proposed models could be used for the entire site. A third model is also specified in Table 1 as the average site velocity structure and was obtained as mean of the other two models.

2.3 Array Configuration

The configuration of the North Haverhill array on the first night of shooting, 17 September 1989 (day 261 UT), is shown in Figure 5. This layout was dictated both by the intended use of the array data, the study of high frequency wave propagation during the Ontario-New York-New England Seismic Experiment, and by the available open land at the site. On 17 September the array consisted of 14 vertical Electro-Tech EV-17 one-second vertical seismometers and 2 EV-17-H horizontal units. The vertical instruments were laid out along two arms having azimuths of 351°59' and 290°34' relative to true North. The northerly arm had a length of 448.0 m while the westerly arm was 341.4 m long. In addition, one vertical instrument was located midway between the arms at a distance of 69.4 meters from the vertex. The two horizontal instruments were collocated at the vertex and oriented to true North and true West, respectively. The location of each sensor, relative to the vertex of the array, is given in Table 2.

After the first series of shots it was determined that the signal from the most northerly instrument, channel 1, was being severely degraded by wind induced noise. This noise was being generated by a line of bushes and trees growing near this seismometer. To reduce this noise source the instrument was moved in towards the vertex by about 100 m. The location of the repositioned seismometer is also given in Table 2. The modified position of this sensor is also shown in Figure 5. Repositioning of the instrument occurred on 23 September (day 267 UT).

Figure 6a shows the beam pattern for the array prior to the repositioning of channel 1 and Figure 6b shows the response following reconfiguration. The responses are plotted in terms of linear wavenumber given by 1/wavelength. As can be seen from these figures, while there is some minor change in the response function in the lowest

Table 1. Velocity models for the North Haverhill array site.

Layer		North Arm			West Arm			Average Model		
Depth (m)	Thick. (m)	V_p (m/sec)	V_s (m/sec)	SD(V_s) (m/sec)	V_p (m/sec)	V_s (m/sec)	SD(V_s) (m/sec)	V_p (m/sec)	V_s (m/sec)	SD(V_s) (m/sec)
0.0	2.5	559.3	322.7	44.1	574.6	331.5	74.4	567.0	327.1	43.2
2.5	2.5	584.3	337.1	34.7	676.6	390.4	59.3	630.5	363.8	34.3
5.0	2.5	836.5	482.6	53.9	801.3	462.3	57.6	818.9	472.5	39.4
7.5	2.5	816.5	471.0	42.6	864.8	498.9	51.6	840.7	485.0	33.5
10.0	2.5	1045.9	603.4	51.4	1158.5	668.4	64.4	1102.2	635.9	41.2
12.5	2.5	1284.5	741.1	46.7	1365.0	787.5	67.4	1324.8	764.3	41.0
15.0	2.5	1415.9	816.9	43.2	1444.8	833.6	64.2	1430.0	825.3	38.7
17.5	2.5	1474.8	850.8	36.9	1461.3	843.0	54.0	1468.1	846.9	32.7
20.0	5.0	1504.8	868.1	40.8	1478.9	853.2	66.9	1491.9	860.7	39.2
25.0	5.0	1543.0	890.2	19.1	1494.9	862.5	36.0	1519.0	876.4	20.4
30.0	5.0	1642.7	947.7	11.5	1579.8	911.4	21.6	1611.3	929.6	12.2
35.0	5.0	1760.1	1015.4	11.0	1704.1	983.1	18.9	1732.1	999.3	10.9
40.0	5.0	1881.6	1085.5	8.7	1839.0	1061.0	14.2	1860.3	1073.3	8.3
45.0	5.0	2003.8	1156.0	5.8	1975.0	1139.4	9.5	1989.4	1147.7	5.6
50.0	10.0	2125.2	1226.1	5.8	2104.7	1214.3	9.8	2115.0	1220.2	5.7
60.0	-	2241.1	1293.0	2.9	2232.8	1288.1	5.0	2237.0	1290.6	2.9

Table 2. North Haverhill Seismic Array Sensor Configuration

Sensor	EAST (m)	NORTH (m)	Z (m)	Range (m)
1-V	-62.5	443.6	170.4	448.0
1-V*	-47.6	338.1	170.6	341.4
2-V	-33.7	239.0	172.1	241.4
3-V	-18.1	128.2	173.6	129.5
4-V	-9.7	68.8	174.4	69.5
5-V	-5.2	36.9	174.9	37.3
6-V	-2.8	19.8	175.3	20.0
7-V	0.0	0.0	175.5	0.0
8-N	0.0	0.0	175.5	0.0
9-W	0.0	0.0	175.5	0.0
10-V	-18.7	7.0	175.3	20.0
11-V	-34.9	13.1	174.8	37.3
12-V	-65.1	24.4	174.2	69.5
13-V	-121.3	45.5	173.1	129.5
14-V	-226.0	84.8	169.4	241.4
15-V	-319.7	119.9	163.3	341.4
16-V	-43.9	53.8	174.2	69.5

* Location following repositioning on 23 September.

contour levels, the change resulting from the reconfiguration is not substantial.

2.4 Array Instrumentation

Data from the array were digitally recorded by the GL developed Geophysical Data Acquisition System (GDAS) [*Blaney*, in prep. 1990], an upgraded version of the GDAS acquisition system previously described by Von Glahn [1980]. The GDAS sampled the array at the rate of 100 samples per second per channel and was recorded either on floppy disk or to 9-track magnetic tape. Anti-aliasing protection was provided by the application to the analog signal of an 2-pole Butterworth filter with a corner frequency of 100 Hz followed by a 6-pole Butterworth filter with a corner at 34.3 Hz. Amplification of the signal was also performed in two stages prior to digitization. During the experiment, the pre-amplification level was set, by hardware, at either a nominal gain of 1000, low gain, or 2000, high gain. Digitization was performed with 15-bit accuracy.

System response was obtained *in-situ* by application of a known current to the calibration coils of the seismometers. Estimates of the full system response, due both to the instrument and signal conditioning hardware, were obtained by minimizing the least squared error between the observed calibration pulses and pulses determined from theoretical models of the system. Table 3 lists the sensor response parameters as determined for the two gain settings. A typical system response function is displayed in Figure 7, in this case for the sensor on channel 7, the vertical seismometer at the vertex of the array.

Time reference for tagging the sampled data was obtained from a GDAS internal clock. This clock was set prior to any recording with reference to a Geo-stationary Orbiting Environmental Satellite (GOES) time code receiver. Residual timing errors were obtained by cross-correlating the GOES and GDAS internal clock pulses. Over any particular recording window, it was found that the relative error between the GOES and the internal clocks was stable within 1 msec or 1/10 of a sample interval.

During the post-experiment configuration tests, it was found that the GDAS sampling software introduced a 205 msec advance on the data time tag. In other words, data tagged as having been taken at t_o sec was actually taken at t_o + 0.205 sec. Thus, all times taken from the GDAS timing information must be increased by a total of 205 msec plus the residual error for the particular shot window to correct to Universal Time. Table 4 lists the residual timing errors for each of the eight shot windows during the experiment.

3. DESCRIPTION OF THE EXPERIMENT

A total of 35 detonations were carried out at 20 shot points distributed at 30 to 35 km intervals along the 650 km profile of the experiment and at three off-line sites, as shown in Figure 1. The locations of the shot points are listed in Table 5 along with the size of each shot and the range and azimuth from the array and the shot time of each detonation. Each event is identified by a combination of a number, 1 through 23 and a letter, either A, B, or C. The number represents the shot point, as labeled in Figure 1, and the letter identifies the sequence of the shot at that shot point. As an example, the third

Table 3. Seismometer Response Parameters

Sensor	Natural Frequency (Hz)	Damping (%)	High Gain Sensitivity 10^6V/(m/s)	Low Gain Sensitivity 10^5V/(m/s)
1-V	0.932	0.698	1.1004	5.2335
2-V	0.966	0.647	1.1251	5.3505
3-V	1.008	0.618	1.0757	5.1159
4-V	0.931	0.662	1.0703	5.0901
5-V	0.951	0.713	1.1641	5.5360
6-V	0.937	0.673	1.1395	5.4191
7-V	0.936	0.737	1.1327	5.3866
8-N	1.004	0.642	1.1880	5.6499
9-W	0.981	0.639	1.2189	5.7970
10-V	0.975	0.625	1.1018	5.2401
11-V	0.951	0.704	1.1021	5.2411
12-V	0.936	0.726	1.1279	5.3638
13-V	0.938	0.718	1.1225	5.3384
14-V	0.924	0.747	1.1507	5.4722
15-V	0.923	0.694	1.1321	5.3841
16-V	0.922	0.655	1.0821	5.1464

Table 4. Residual Timing Errors for Experiment Shot Windows

Sequence No.	Window Time (UT)	Residual Error[1] (msec)	Total Error[2] (msec)
1	261:04:00	+19	+224
2	261:06:00	+19	+224
3	261:08:00	+19	+224
4	268:04:00	-06	+199
5	268:06:00	-06	+199
6	268:08:00	-06	+199
7	274:04:00	-36	+169
8	274:06:00	+87	+292

[1] Residual error between GOES receiver and GDAS internal clocks. Positive indicates GDAS clock is late relative to GOES receiver.

[2] Total error includes software induced time shift. Positive indicates error to be added to times given by GDAS system.

Table 5. Shot Parameters for the Experiment

Shot ID	Shot Time Day:Hr:Mn:Sec	Shot Location Lat(N)	Long(W)	Elev. (m)	Size (kg)	Range (km)	Azimuth (° from N)
1A	261:06:04:0.006	44°35.41'	69°44.77'	95	2091	188.7	71.7
2A	261:04:00:0.006	44°33.80'	70°02.67'	122	1012	165.2	70.3
3A	261:08:00:0.011	44°27.53'	70°31.36'	277	1021	125.6	69.8
4A	261:06:02:0.010	44°24.69'	70°58.18'	317	987	90.6	65.6
4B	268:08:06.0.011	44°24.69'	70°58.18'	317	1225	90.6	65.6
5A	261:04:02:0.009	44°20.17'	71°23.10'	516	998	57.3	59.9
6A	261:06:00:0.006	44°16.86'	71°49.79'	329	907	26.5	32.2
7A	261:04:04:0.006	44°10.71'	72°14.19'	460	1225	21.3	301.2
7B	268:06:00:0.009	44°10.71'	72°14.19'	460	1225	21.3	301.2
8A	268:04:00:0.009	44°09.05'	72°34.60'	433	907	46.0	280.2
9A	268:04:02:0.006	44°04.41'	72°55.96'	671	907	73.8	269.8
10A	261:08:04:0.010	44°03.22'	73°23.19'	35	1361	110.1	269.0
10B	268:06:06:0.006	44°03.22'	73°23.19'	35	907	110.1	269.0
10C	274:06:06:0.005	44°03.22'	73°23.19'	35	1361	110.1	269.0
11A	268:08:02:0.006	43°59.53'	73°39.67'	287	975	132.5	266.4
12A	268:04:04:0.007	43°56.26'	73°58.96'	535	953	158.7	265.0
13A	268:06:04:0.007	43°58.08'	74°15.69'	524	1043	180.6	266.9
14A	261:04:08:0.006	43°59.97'	74°29.27'	530	1361	198.4	268.3
14B	268:08:00:0.007	43°59.97'	74°29.27'	530	1247	198.4	268.3
14C	274:04:06:0.009	43°59.97'	74°29.27'	530	1134	198.4	268.3
15A	274:06:04:0.006	44°09.34'	75°00.95'	427	816	240.2	273.1
16A	274:06:02:0.007	44°14.64'	75°31.70'	175	885	281.3	275.0
17A	268:06:02:0.010	44°17.83'	75°55.55'	94	1157	313.2	275.8
17B	274:04:04:0.009	44°17.83'	75°55.55'	94	272	313.2	275.8
18A	274:04:01:59.990	44°18.08'	76°43.11'	140	907	376.3	275.4
19A	274:05:59:59.996	44°20.11'	77°12.27'	180	907	415.0	275.7
20A	268:04:07:59.970	44°28.63'	77°39.49'	0	1361	451.8	277.6
20B	274:04:59:59.969	44°28.63'	77°39.49'	0	907	451.8	277.6
21A	268:08:04:0.007	43°03.42'	72°56.29'	710	907	136.1	213.7
22A	261:04:06:0.008	43°14.17'	71°51.53'	325	907	94.5	172.7
22B	268:04:06:0.007	43°14.17'	71°51.53'	325	907	94.5	172.7
23A	261:08:02:0.010	43°26.95'	70°40.31'	79	1030	128.2	122.7

detonation at shot point 10 is designated as shot 10C.

With the exception of shot point 20, all shots were carried out in boreholes between 48 and 55 m deep. Each hole was 20 cm in diameter, cased to bedrock, and continued at least 3 meters into competent rock. Shot point 20 was unique in that the shots at this location were fired underwater in an abandoned quarry.

To allow for the multiple sensor deployments required for the main refraction line the experiment was carried out over three nights, 17, 24, and 29 September. Shooting started at midnight local time, 0400 GMT, to minimize cultural noise during the experiment. Further, to simplify logistics for the shooters, the shots on each night were broken into two or three windows starting on the even hour with subsequent shots at two minute intervals.

The procedure used at the North Haverhill array was to begin recording the array output approximately 2 minutes prior to the hour to obtain an ambient noise sample for the shot window. Recording was continued for at least 4 minutes following the detonation of the last shot scheduled for the particular window to allow for signal propagation and to provide post-shot noise samples. This typically required continuous recording for 14 minutes and recording was done to 9 track tape. In addition to recording the shot signals, high and low gain calibrations were run each shooting night.

4. ARRAY RECORDINGS

Sufficiently high signal to noise levels were achieved at the array for simple visual detection of the signals from all events within 300 km of the array. This included all detonations at shot points 1 through 16 and the fan shots at shot points 21, 22, and 23. Figures 8 through 33 show the instrument response corrected, amplitude normalized traces from each channel of the array as recorded for each of the 26 visually detected events. Instrument response corrections were made over the frequency band of 1.0 to 34.3 Hz and no other processing has been done on this data. These figures show 16 seconds of data including approximately 2 seconds of data proceeding the first arrival for each event.

As discussed in previous sections, in addition to the actual shot recordings, ambient noise samples, calibration pulse outputs and hammer blow data were recorded for the array. Although too numerous to fully display, examples of these data files are shown in Figures 34, 35 and 36. Figure 34 shows a typical pre-shot noise sample. As expected from the proximity of the sensors to tree lines, channels 1 and 15, at the extremes of the array tend to be the noisiest vertical sensor sites with the rms level dropping significantly towards the vertex of the array. Figure 35 shows the voltage output of each channel in the array resulting from a calibration pulse through the high gain system configuration. These signals were used to define the system response functions for each data channel. Figure 36 shows an aligned and stacked hammer blow data file. In this case, the hammer was located at the channel 2 sensor and the hammer accelerometer output replaced the seismometer output. This data file was generated by aligning the hammer strikes, as indicated on the hammer accelerometer traces, in each of four original data files and stacking the remaining channels with the appropriate time shifts. Finally, a 10 Hz highpass filter was applied to the stacked data files. During the hammer blow survey channel 1 exhibited reduced response, likely the result of a sticky mass due to the hammer blow at this site. As the hammer blow survey was completed after the last shot night, this did not cause any problems during the shot windows.

5. DATA ARCHIVE FORMATS

After completetion of the field experiment, the raw data tapes were unpacked into binary data files of 2 minute duration starting on the minute of each scheduled detonation. Further editting was performed on each of these 2 minute window files to obtain the final analysis files for each shot. The actual shot files contain approximately 5 seconds of pre-event noise, the actual shot and several seconds or more of signal following the decay of the coda below the ambient noise. All data files from the experiment, including calibration, gain checks, hammer blow survey and the shot recordings have been archived in several formats and at several stages of processing including the raw data files, where required, deglitched files, and instrument response corrected files. These include DEC RSX-11M and VAX VMS operating system compatible binary formats and an equivalent MS-DOS binary file format. Software for the conversion of either archival form to standard ASCII files is also available or the data can be provided in ASCII format.

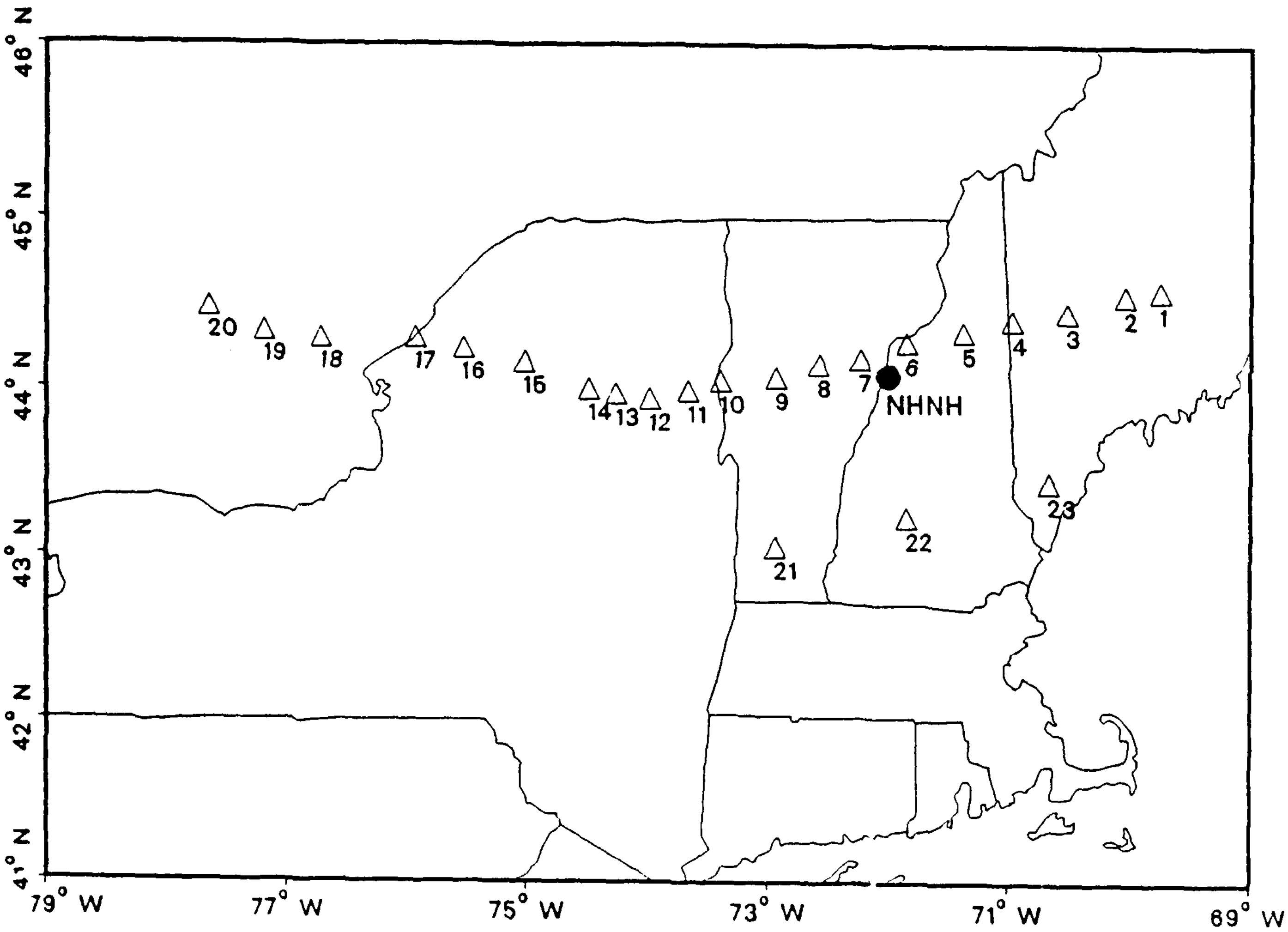

Figure 1. Map of the General Area of Study for the Ontario-New York-New England Seismic Refraction Experiment Showing the Location of the GL Small-Aperture Seismic Array, the Filled Circle Labeled NHNH, and the 23 Shot Points Used During the Experiment (Open Triangles) Labeled with the Associated Shot Numbers.

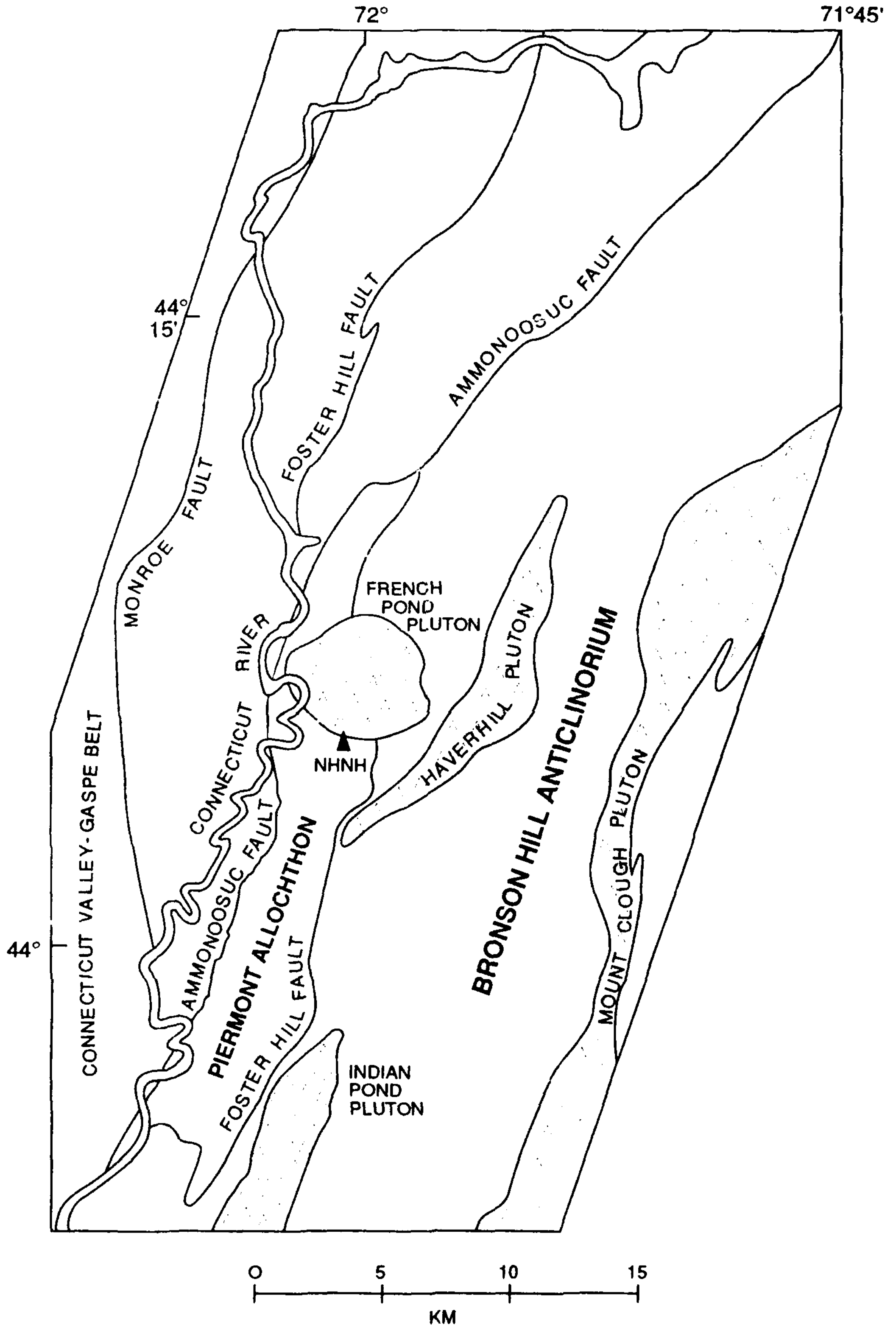

Figure 2. Generalized Geologic Map of the North Haverhill, New Hampshire Area Showing the Geologic Features in the Vicinity of the GL Small-Aperture Array.

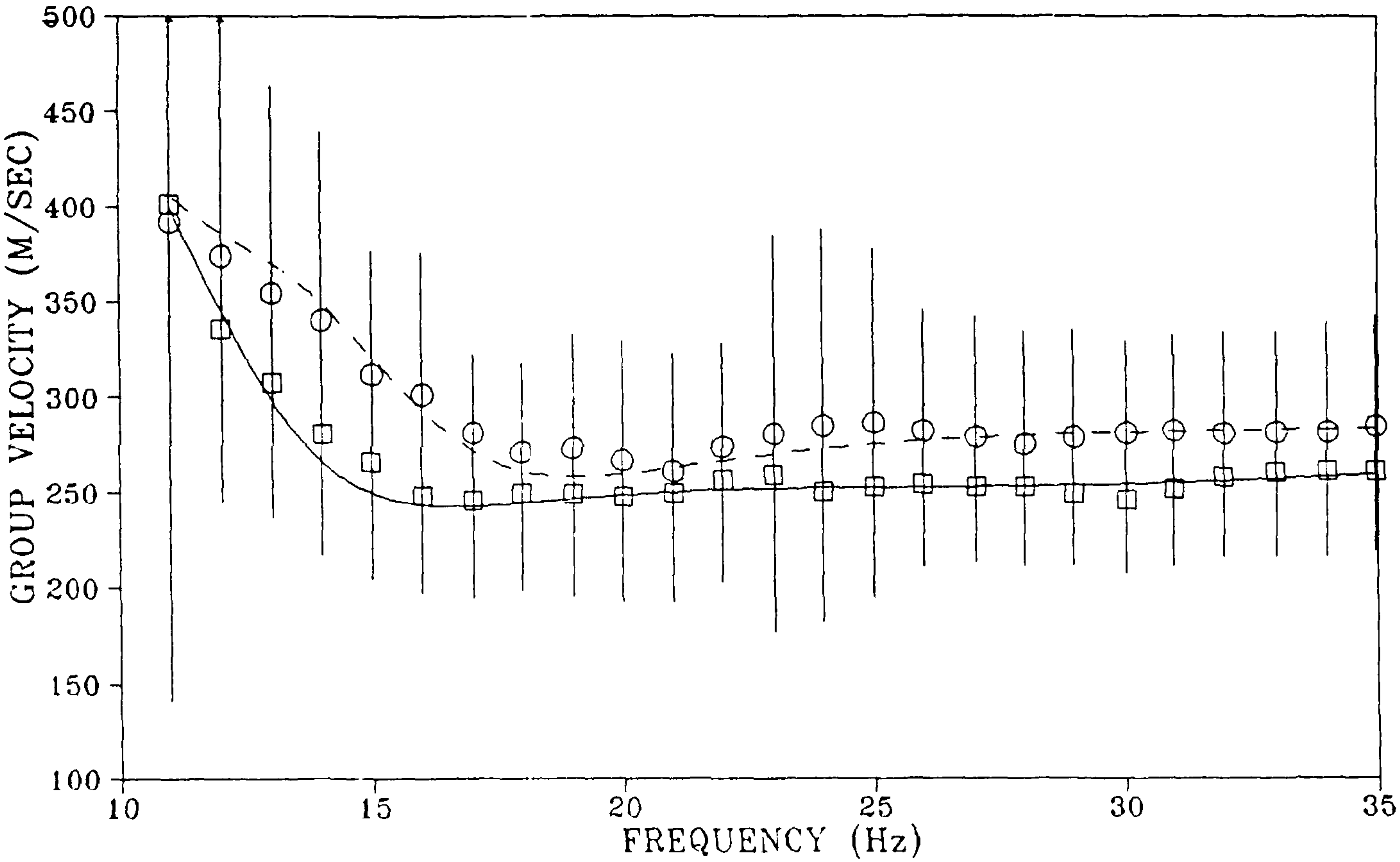

Figure 3. Group Velocity Dispersion Curves for the GL Small-Aperture Array Site Based on Analysis of Hammer Blow Survey Data. The open boxes represent observed data derived from surveys taken along the north arm of the array while the open circles are the observed dispersion curve for the west arm. The lines, solid for north arm and dashed for west arm, represent the theoretical dispersion curves for the velocity structures obtained through inversion.

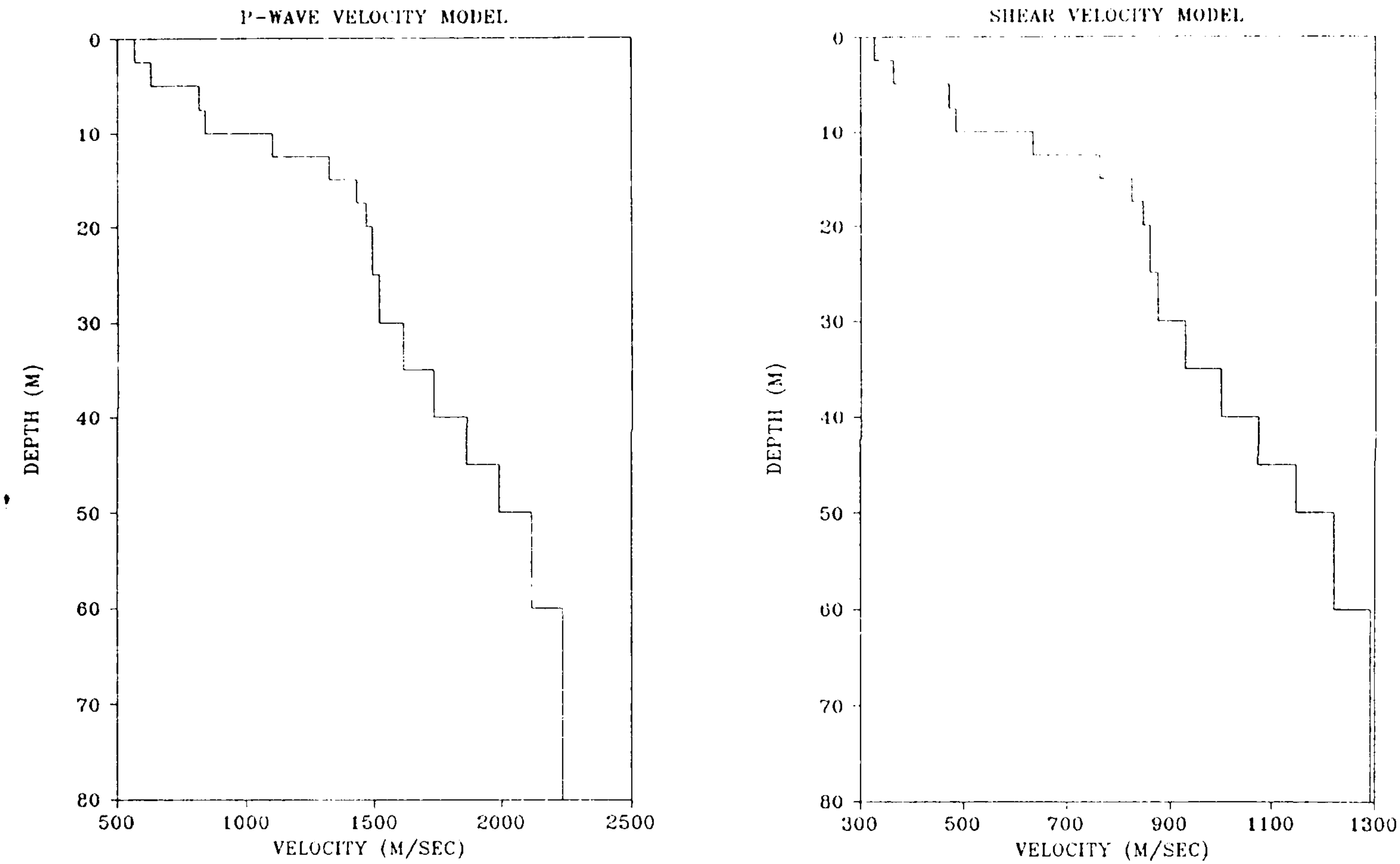

Figure 4. Mean (a) P-wave Velocity and (b) S-wave Velocity Structures for the Inversion of the Group Velocity Dispersion Curves Shown in Figure 3.

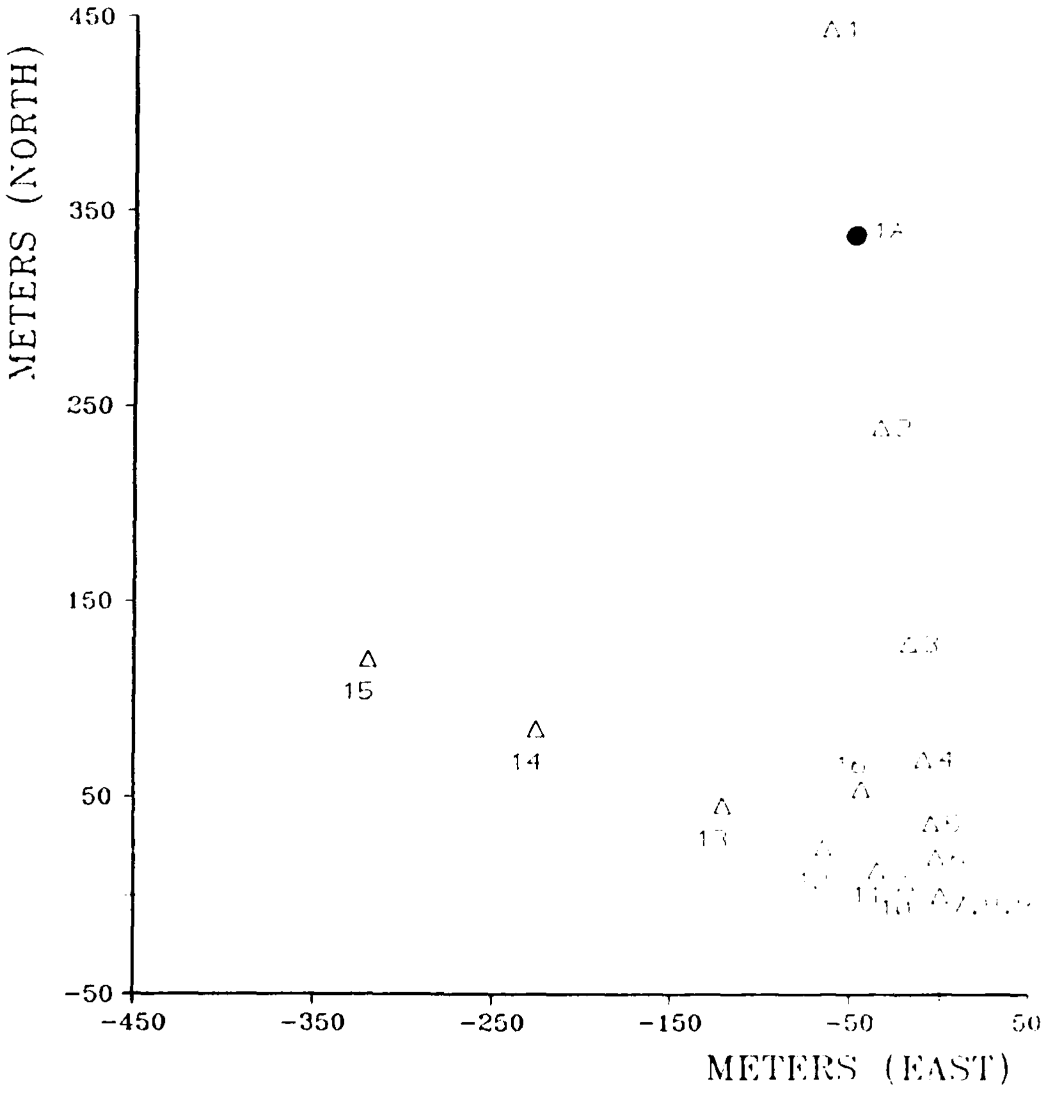

Figure 5. Configuration of the GL North Haverhill, New Hampshire Small-Aperture Array for the Shot Windows on 17 September 1988 (Open Triangles) with the Modified Location of Channel 1 for the Later Shot Windows Shown as a Closed Circle.

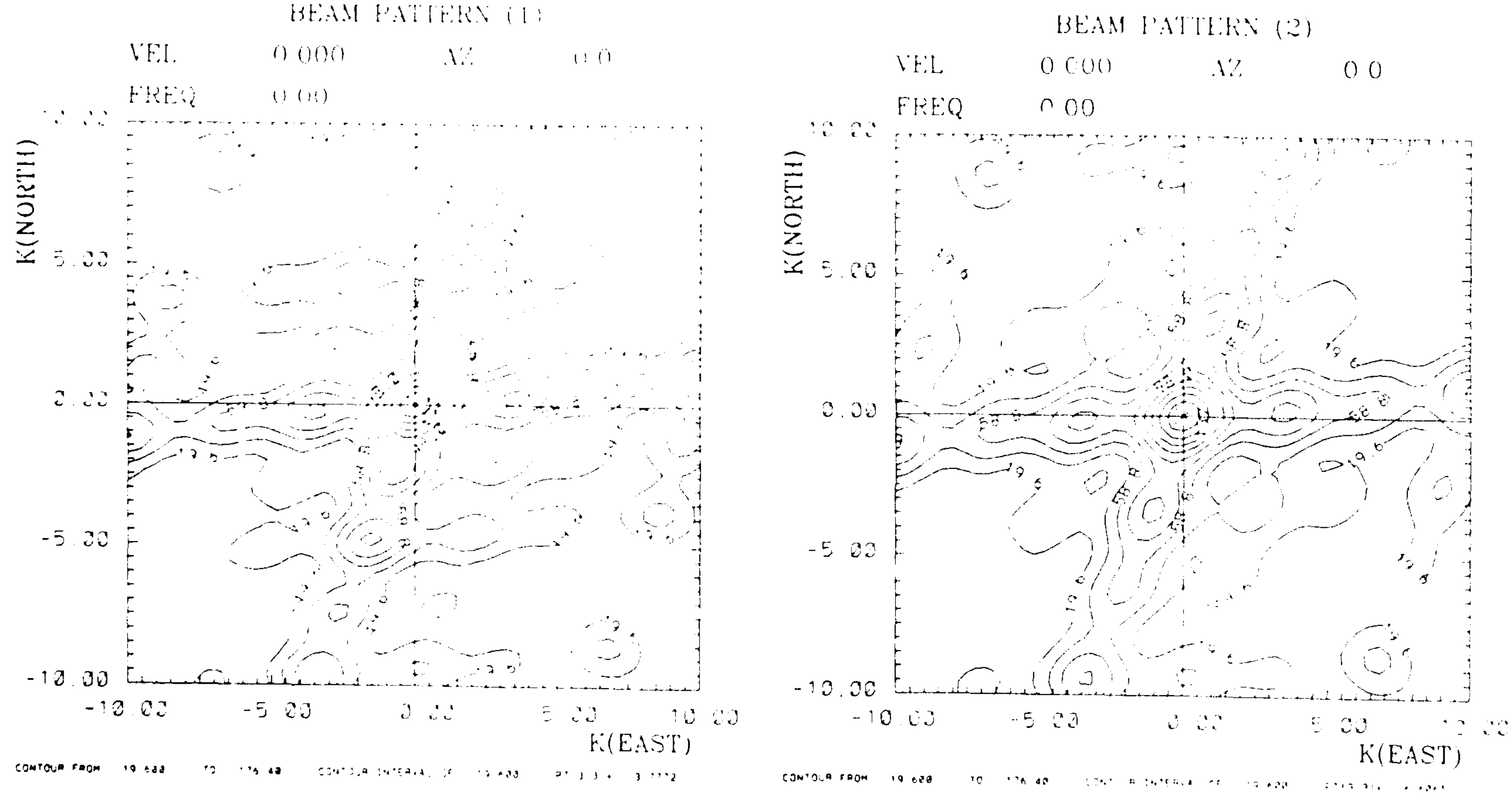

Figure 6. Beam Pattern for the (a) Initial Array Configuration and (b) Following the Repositioning of the Channel 1 Sensor on 23 September. Note that linear wavenumber, 1/wavelength, is used on these plots.

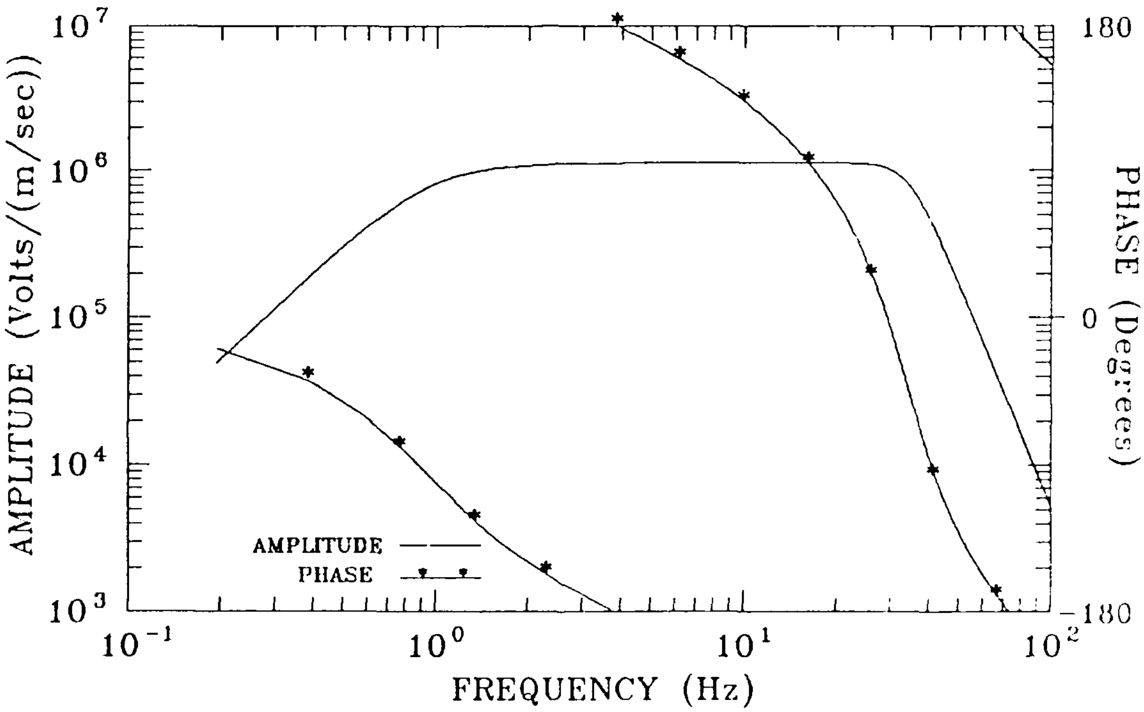

Figure 7. Typical System Response Curve for an Element of the North Haverhill Array When Operating in the High Gain Mode. The plotted response function is for the vertical sensor at the vertex of the array, channel 7.

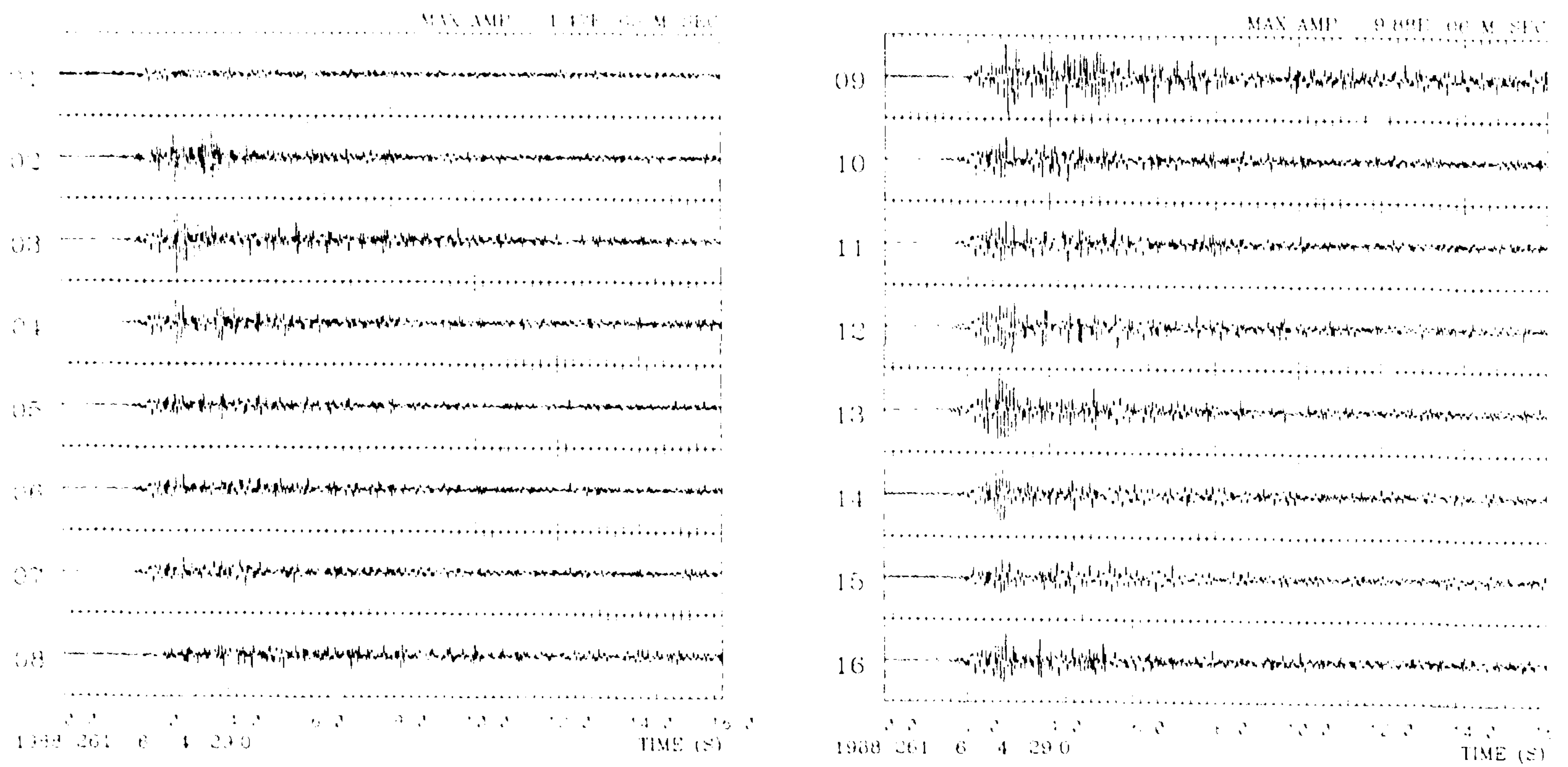

Figure 8. Instrument Response Corrected Traces for Channels 1 Through 8 (a) and 9 Through 16 (b) for Shot 1A as Recorded by the North Haverhill Array.

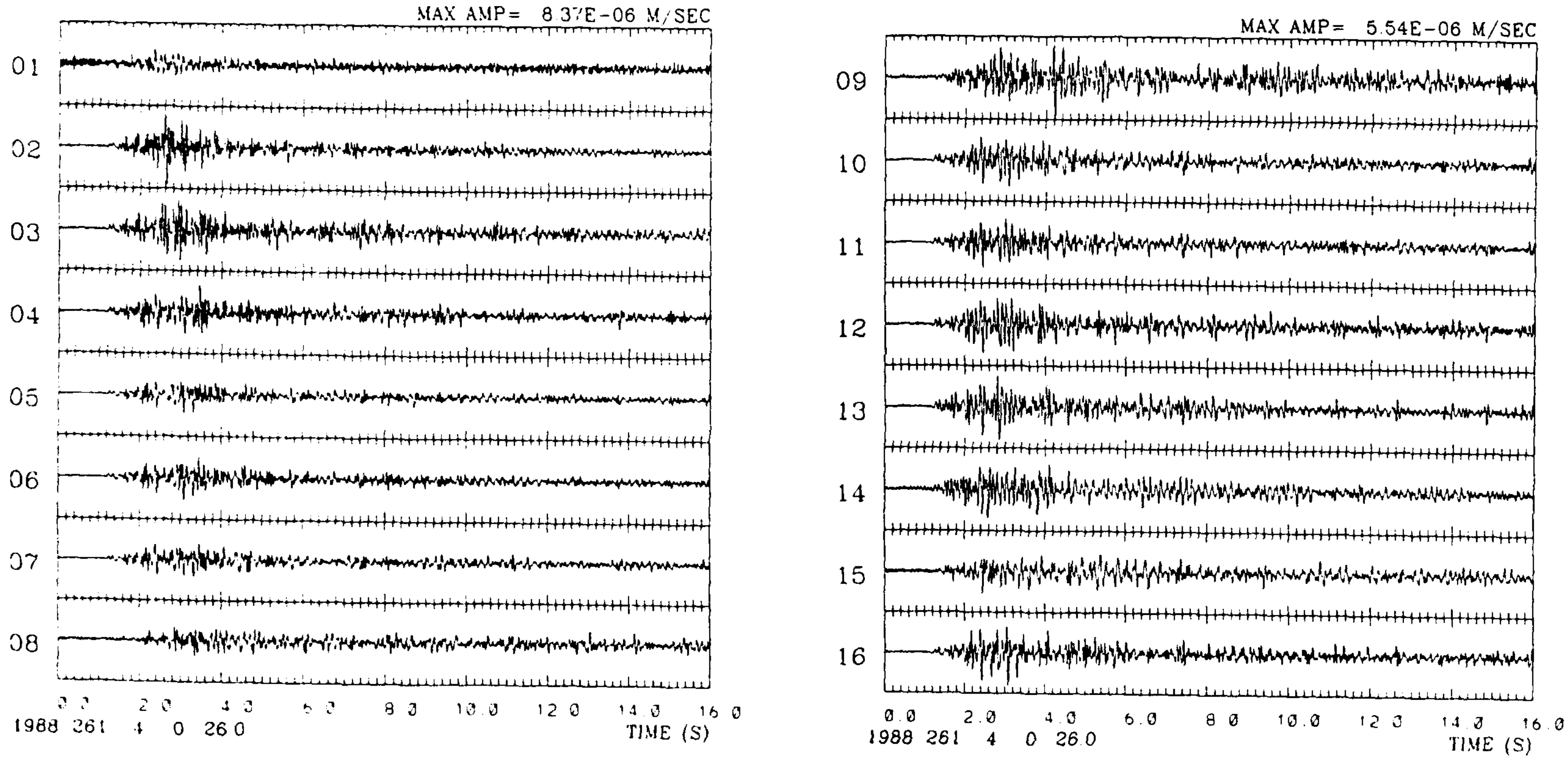

Figure 9. Instrument Response Corrected Traces for Channels 1 Through 8 (a) and 9 Through 16 (b) for Shot 2A as Recorded by the North Haverhill Array.

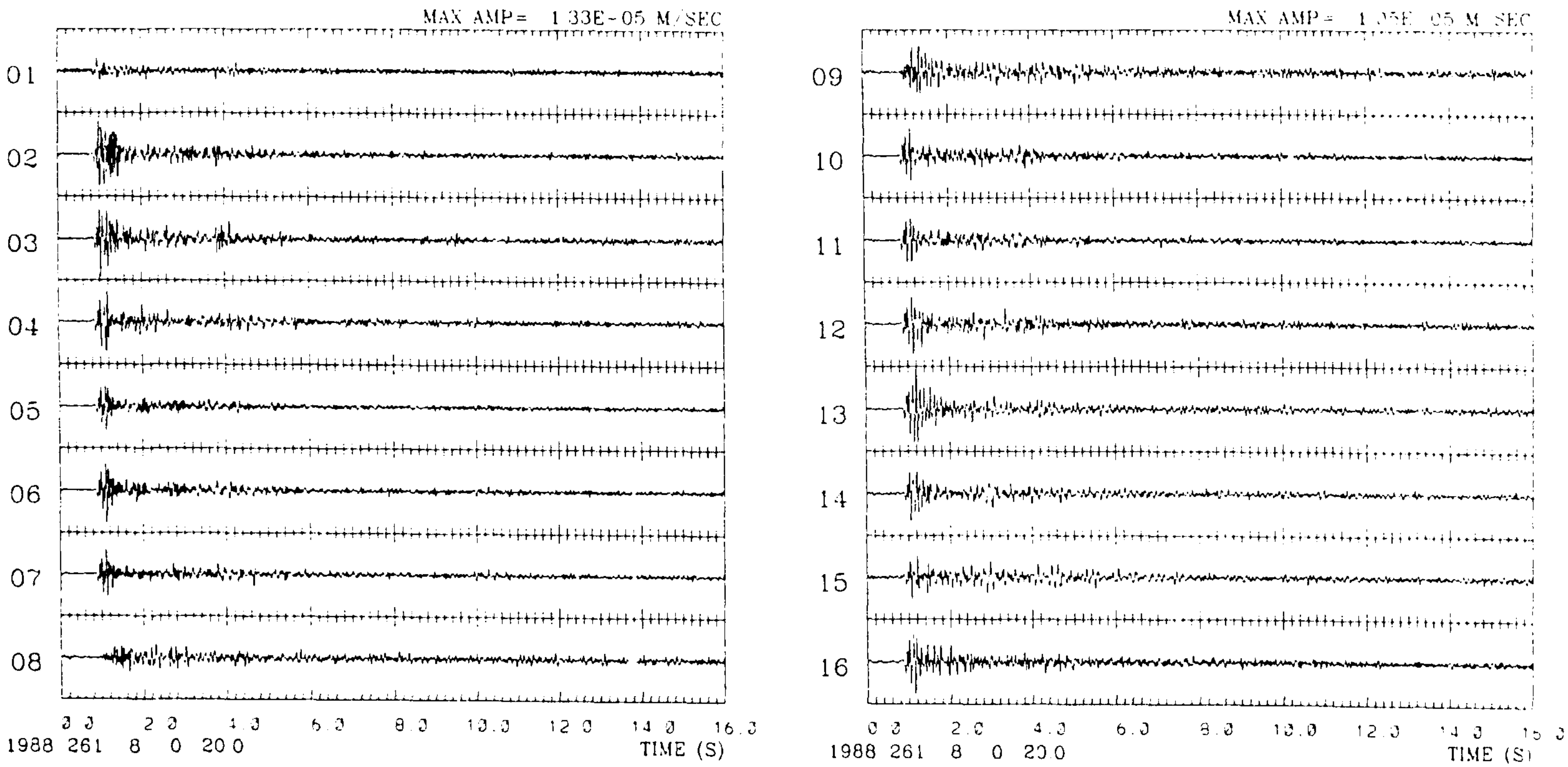

Figure 10. Instrument Response Corrected Traces for Channels 1 Through 8 (a) and 9 Through 16 (b) for Shot 3A as Recorded by the North Haverhill Array.

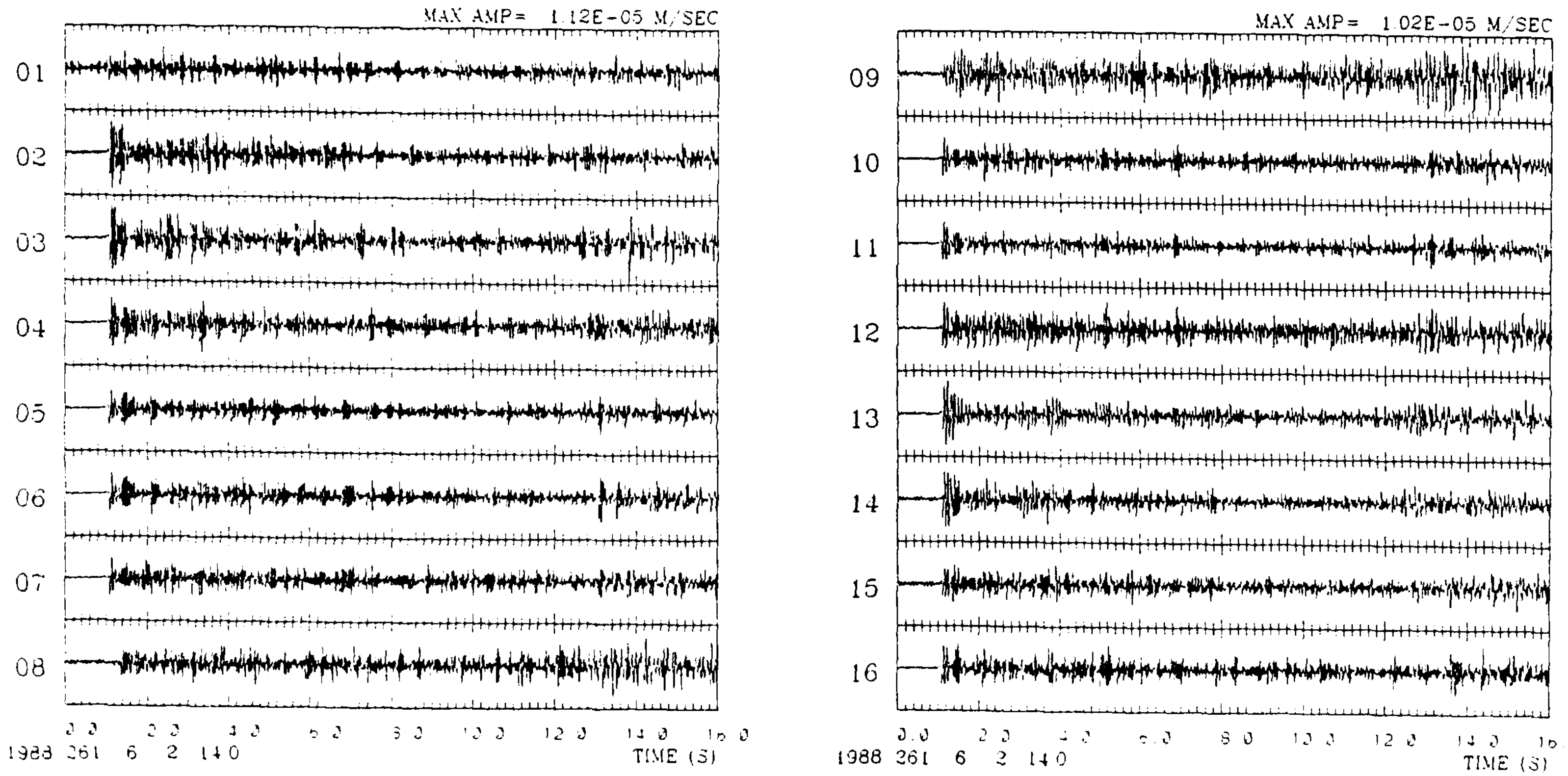

Figure 11. Instrument Response Corrected Traces for Channels 1 Through 8 (a) and 9 Through 16 (b) for Shot 4A as Recorded by the North Haverhill Array.

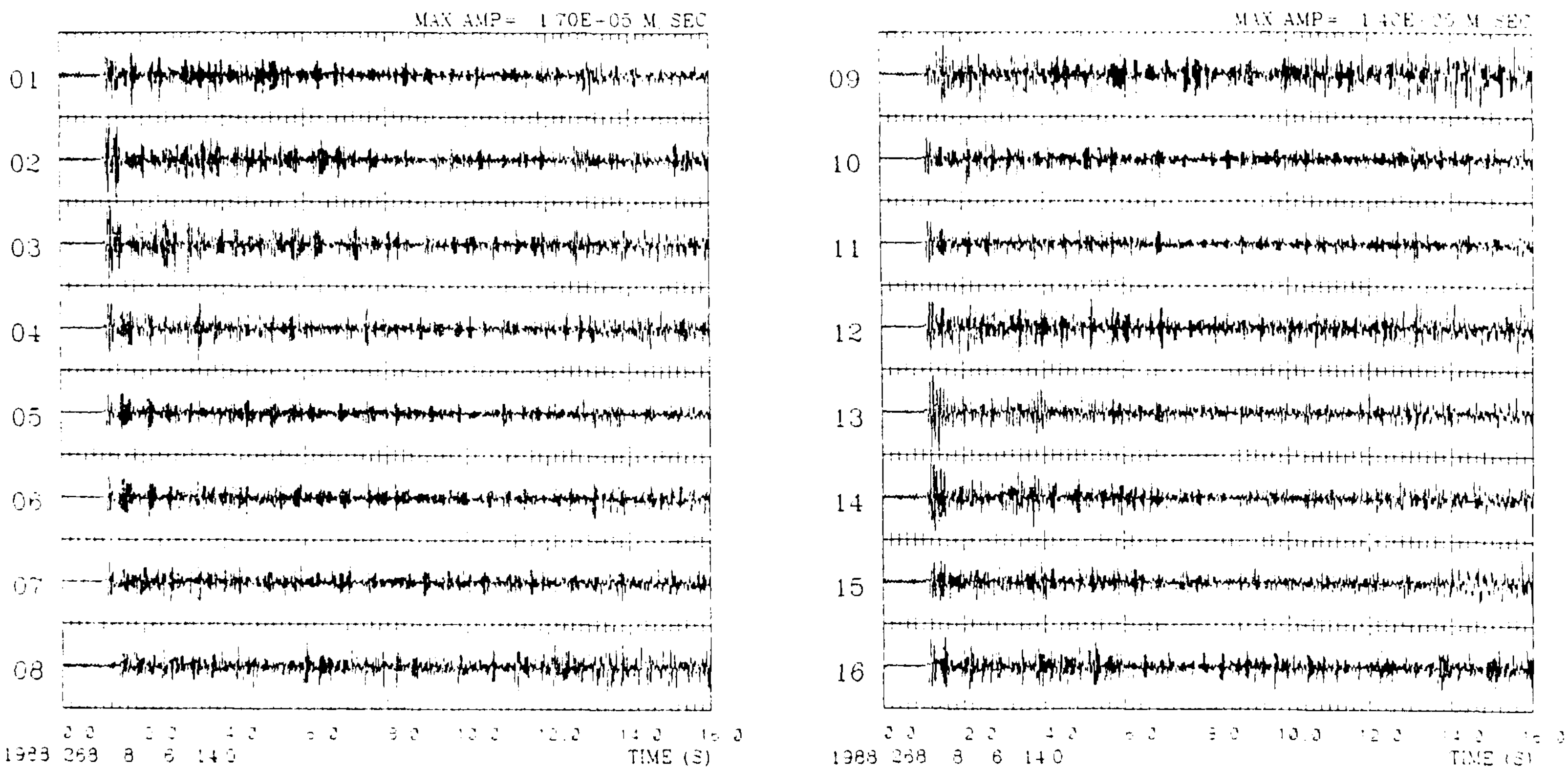

Figure 12. Instrument Response Corrected Traces for Channels 1 Through 8 (a) and 9 Through 16 (b) for Shot 4B as Recorded by the North Haverhill Array.

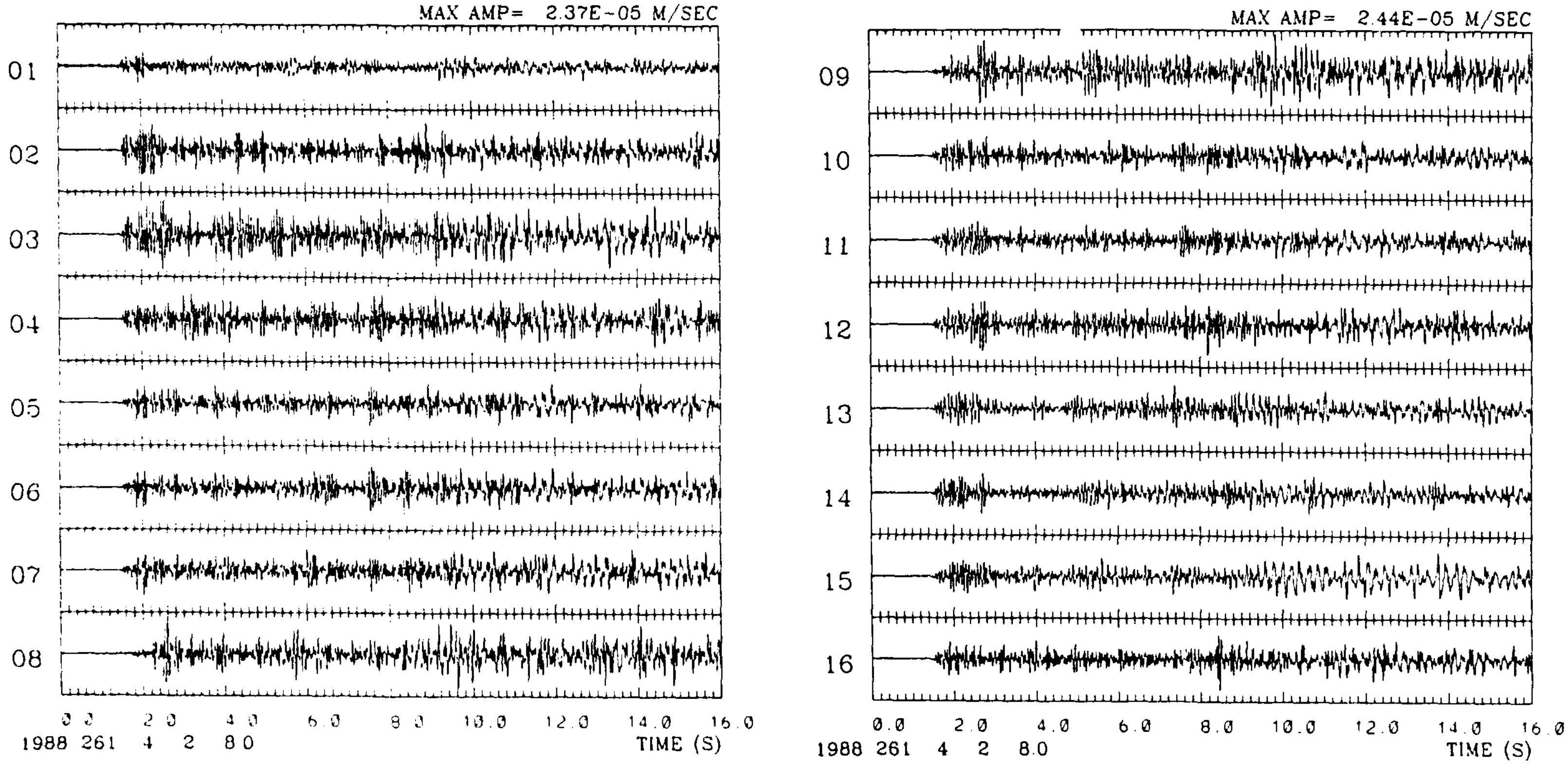

Figure 13. Instrument Response Corrected Traces for Channels 1 Through 8 (a) and 9 Through 16 (b) for Shot 5A as Recorded by the North Haverhill Array.

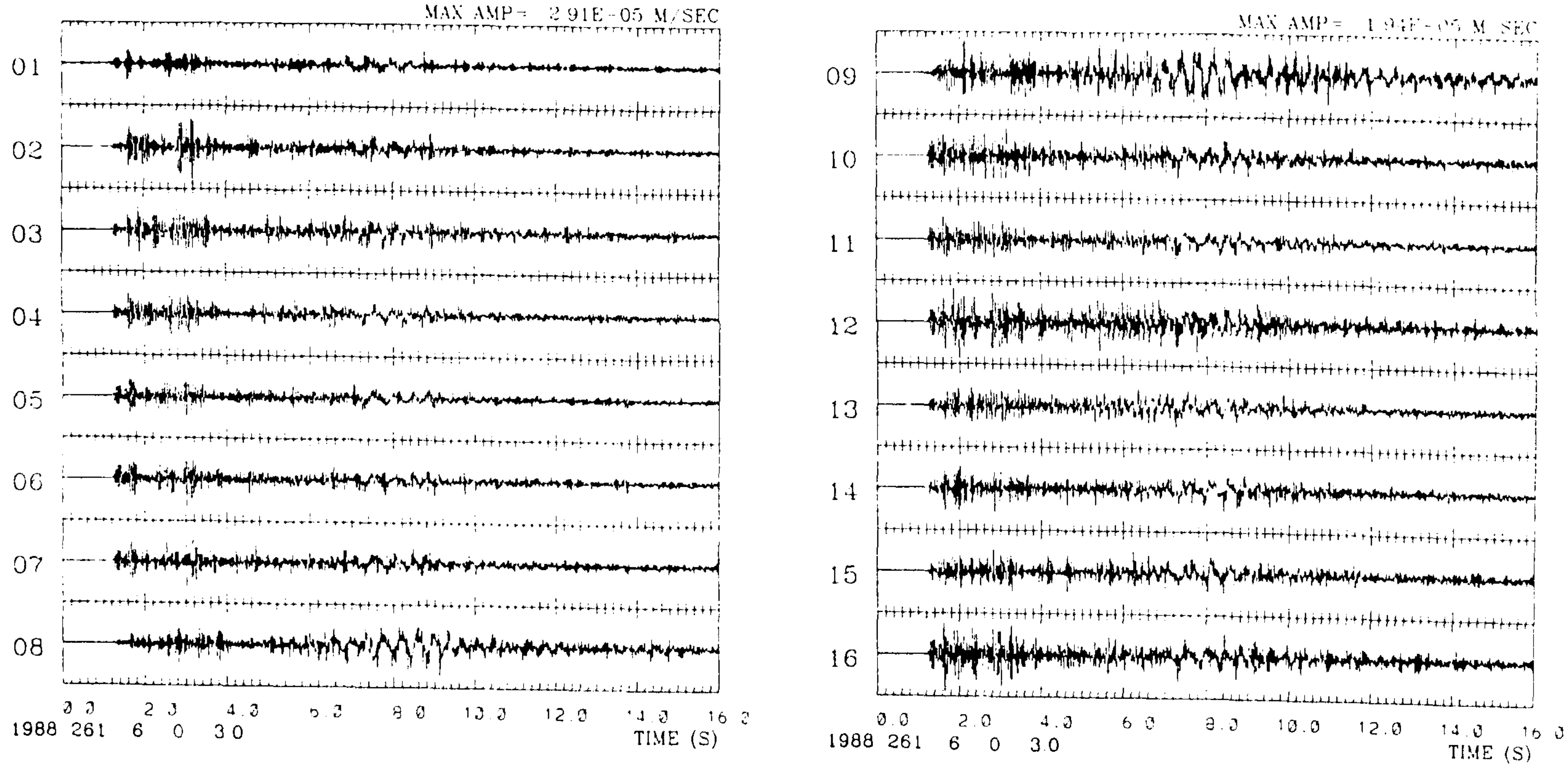

Figure 14. Instrument Response Corrected Traces for Channels 1 Through 8 (a) and 9 Through 16 (b) for Shot 6A as Recorded by the North Haverhill Array.

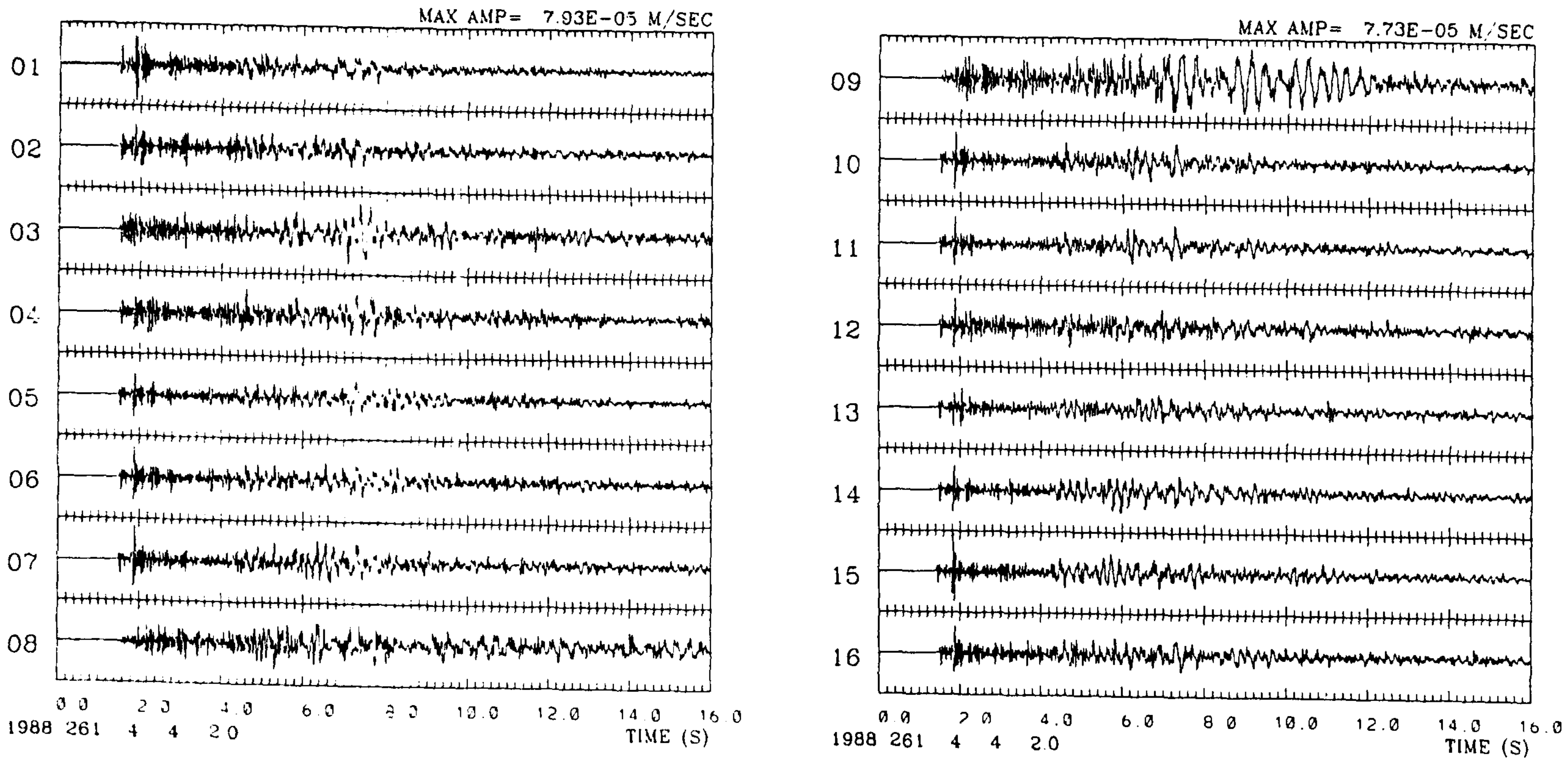

Figure 15. Instrument Response Corrected Traces for Channels 1 Through 8 (a) and 9 Through 16 (b) for Shot 7A as Recorded by the North Haverhill Array.

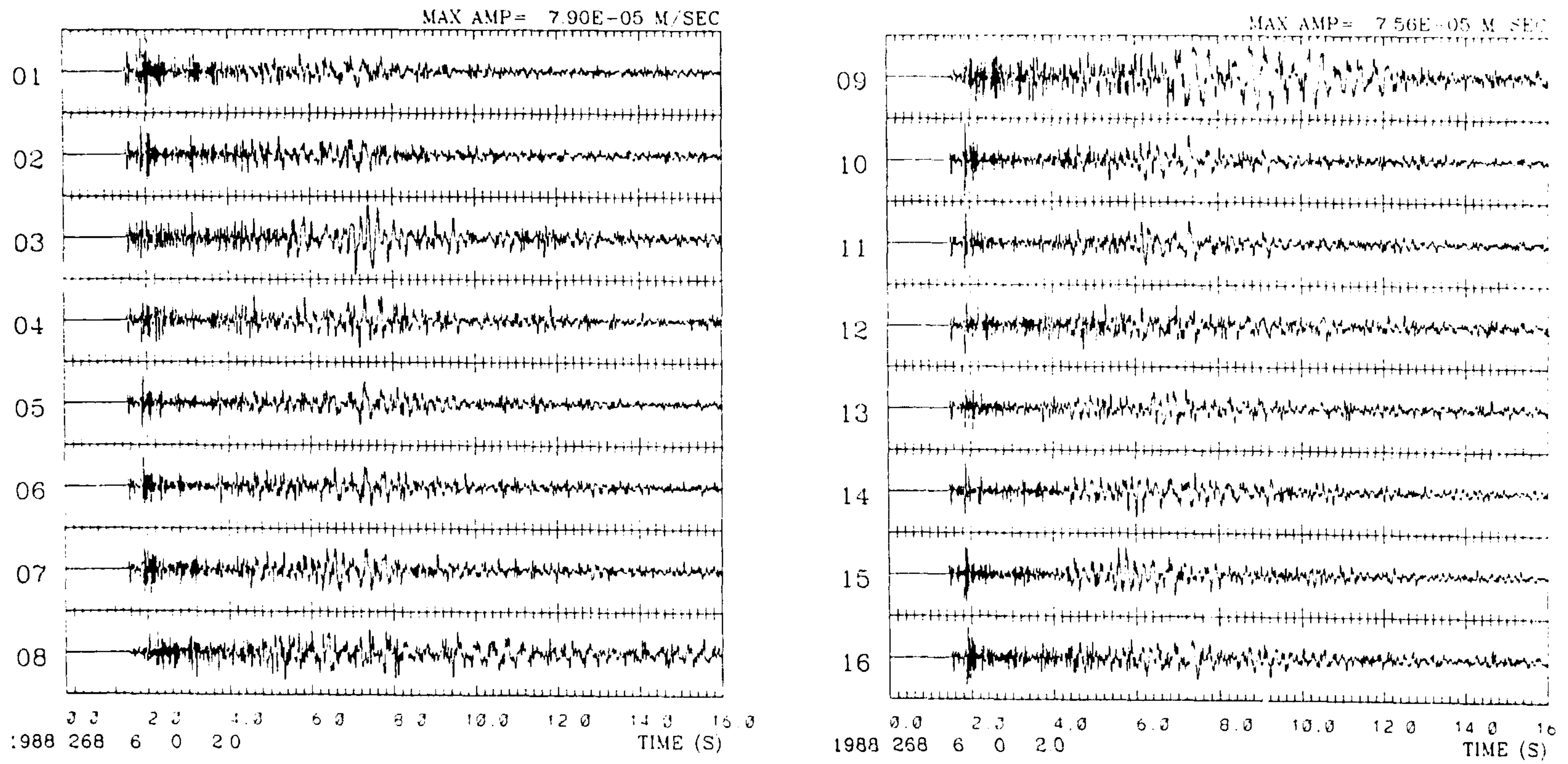

Figure 16. Instrument Response Corrected Traces for Channels 1 Through 8 (a) and 9 Through 16 (b) for Shot 7B as Recorded by the North Haverhill Array.

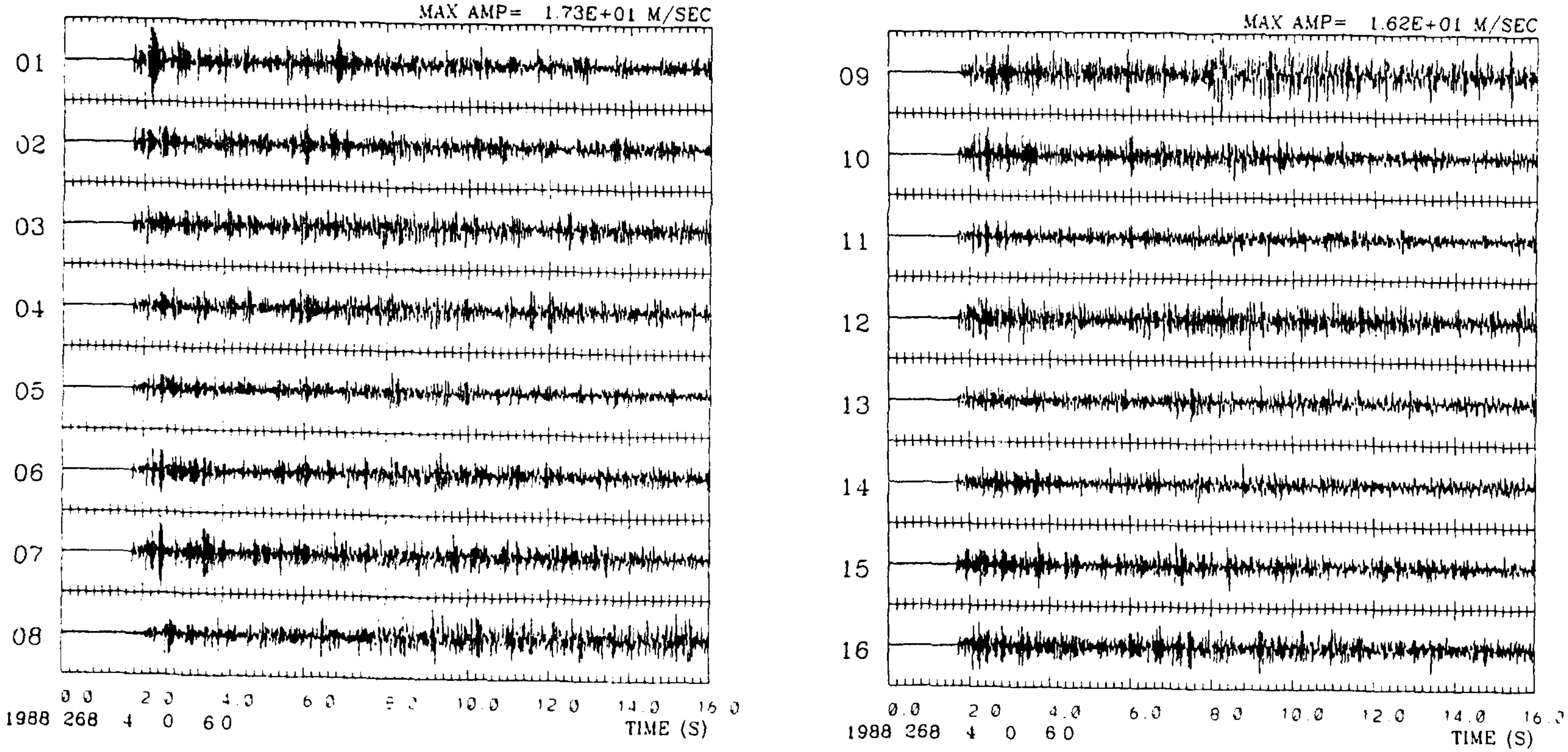

Figure 17. Instrument Response Corrected Traces for Channels 1 Through 8 (a) and 9 Through 16 (b) for Shot 8A as Recorded by the North Haverhill Array.

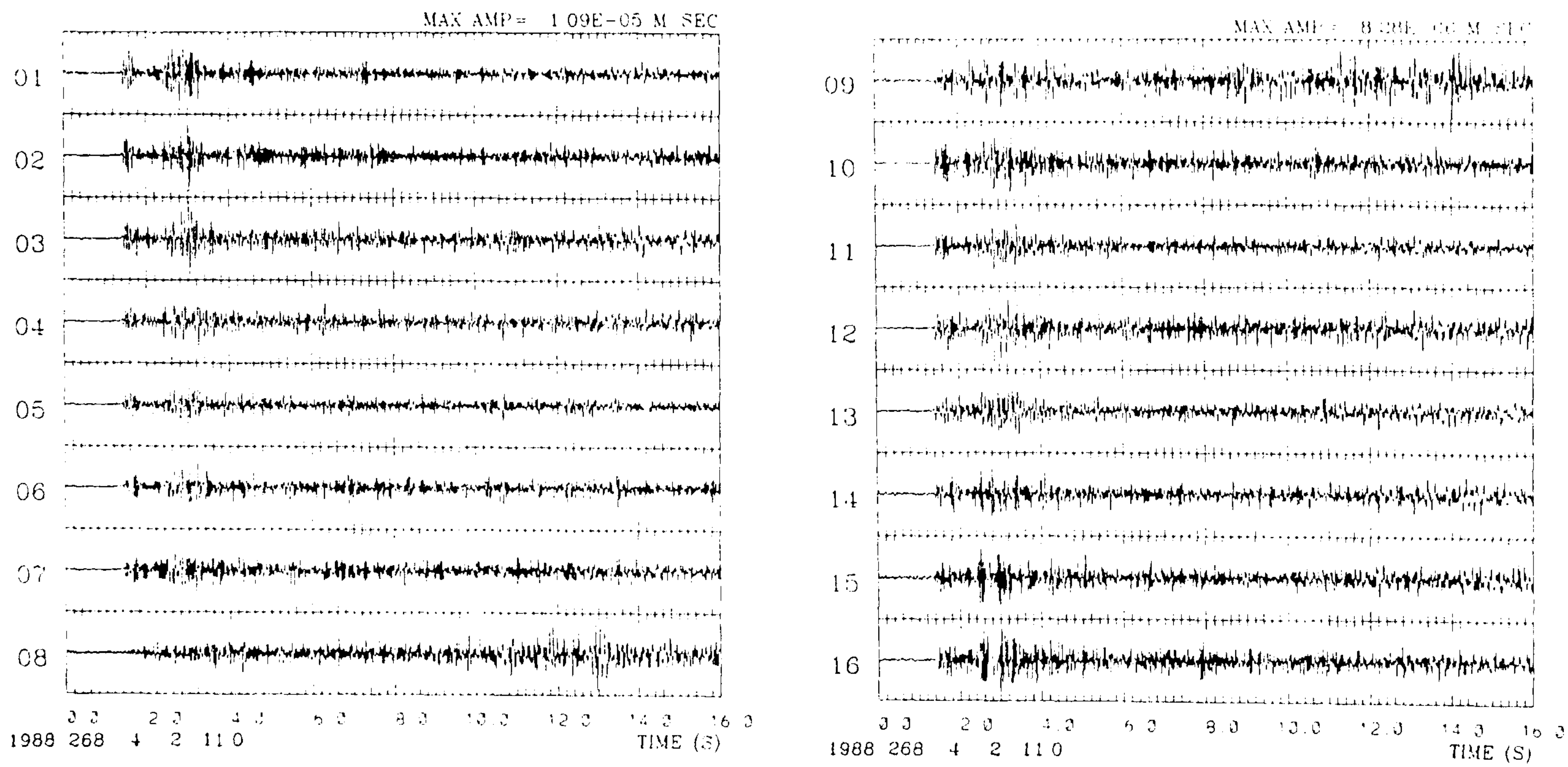

Figure 18. Instrument Response Corrected Traces for Channels 1 Through 8 (a) and 9 Through 16 (b) for Shot 9A as Recorded by the North Haverhill Array.

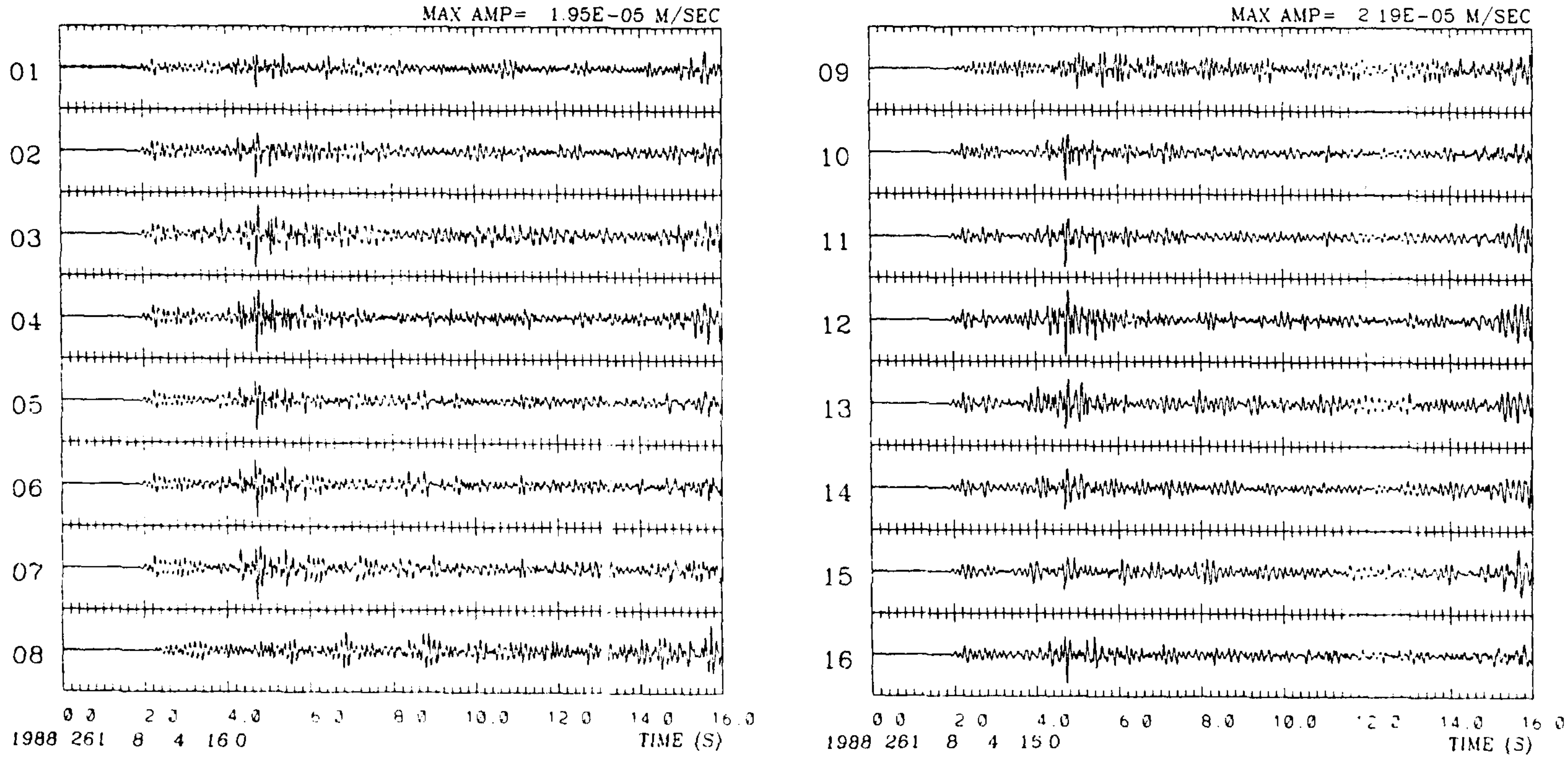

Figure 19. Instrument Response Corrected Traces for Channels 1 Through 8 (a) and 9 Through 16 (b) for Shot 10A as Recorded by the North Haverhill Array.

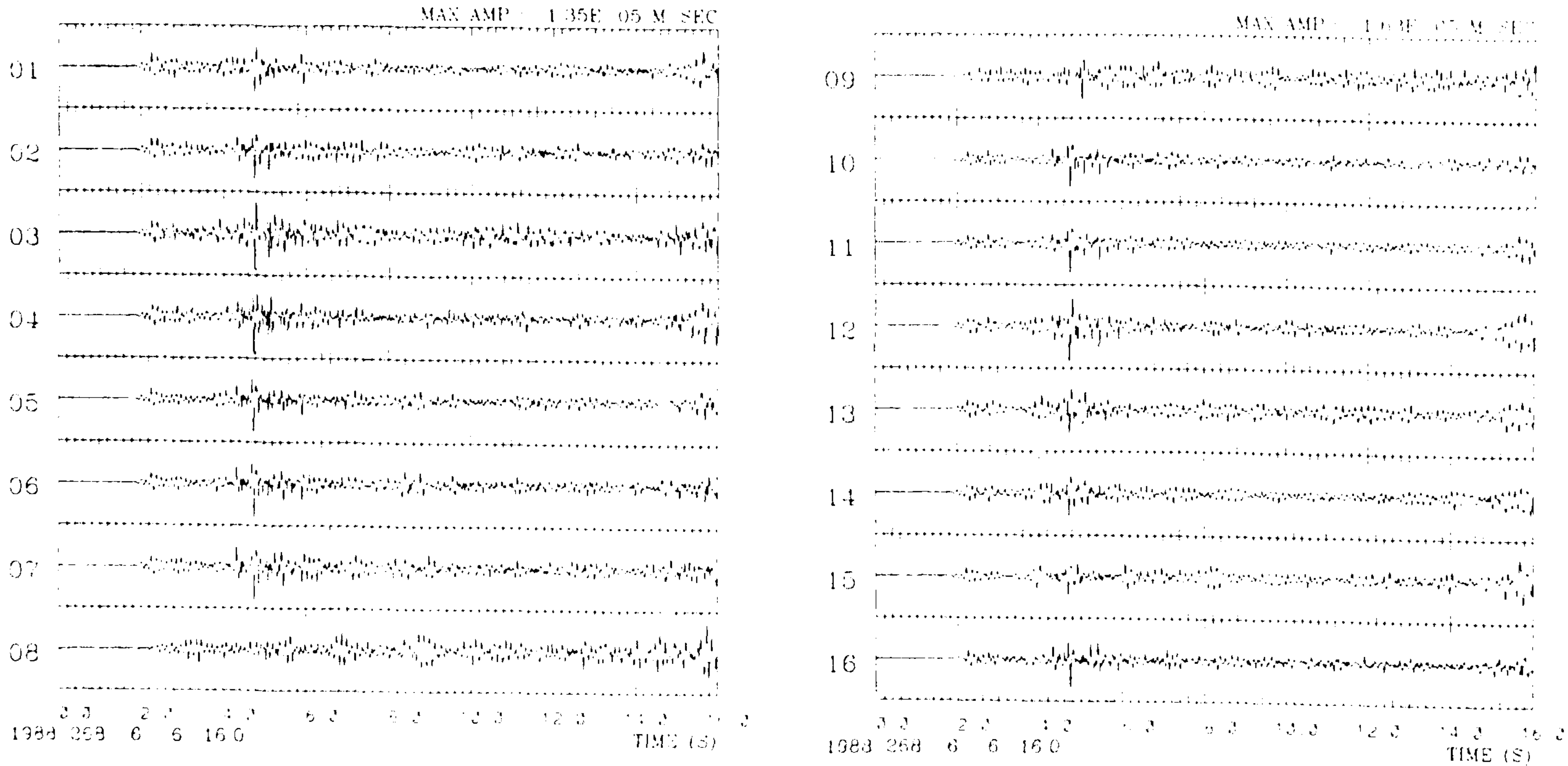

Figure 20. Instrument Response Corrected Traces for Channels 1 Through 8 (a) and 9 Through 16 (b) for Shot 10B as Recorded by the North Haverhill Array.

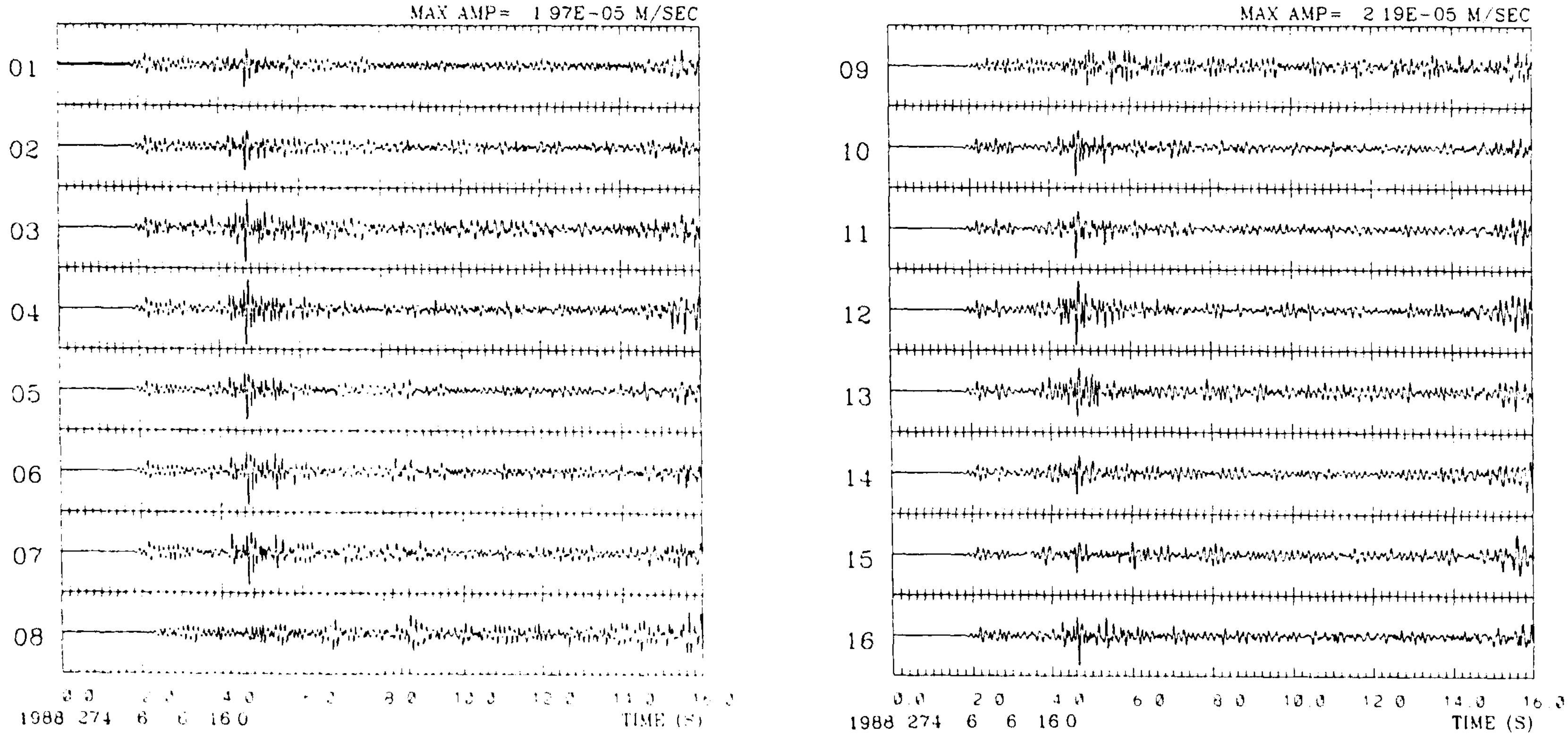

Figure 21. Instrument Response Corrected Traces for Channels 1 Through 8 (a) and 9 Through 16 (b) for Shot 10C as Recorded by the North Haverhill Array.

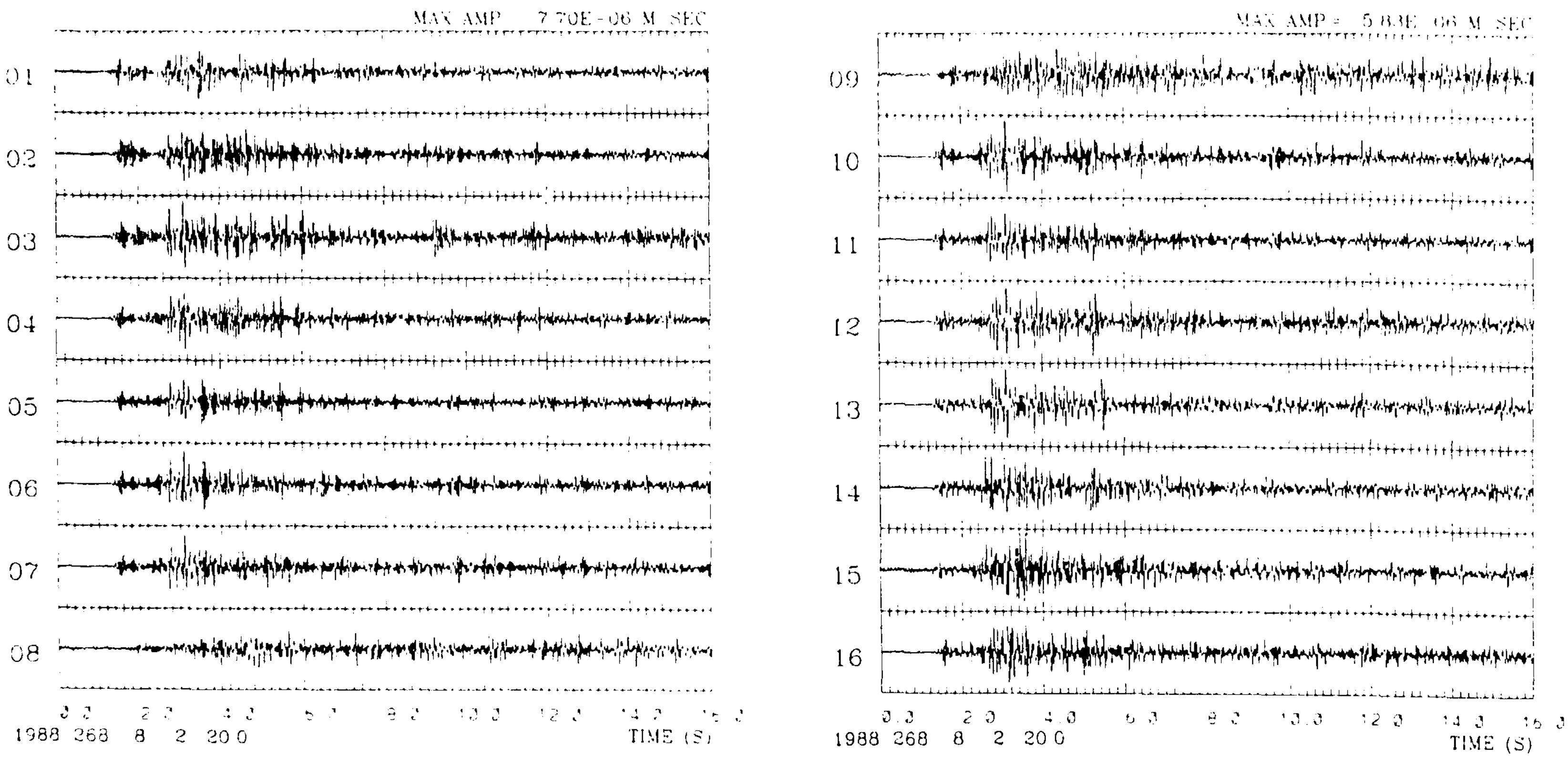

Figure 22. Instrument Response Corrected Traces for Channels 1 Through 8 (a) and 9 Through 16 (b) for Shot 11A as Recorded by the North Haverhill Array.

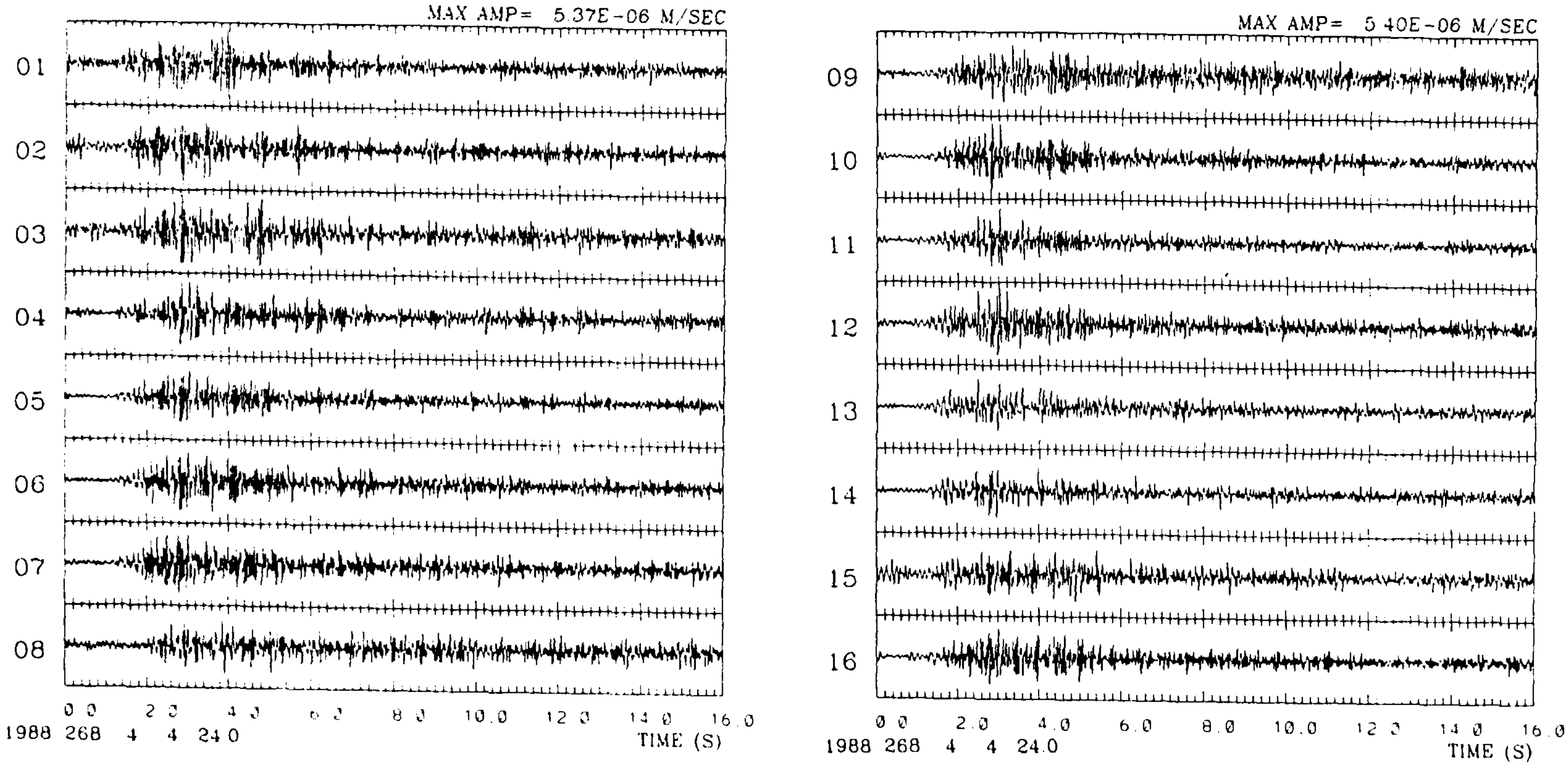

Figure 23. Instrument Response Corrected Traces for Channels 1 Through 8 (a) and 9 Through 16 (b) for Shot 12A as Recorded by the North Haverhill Array.

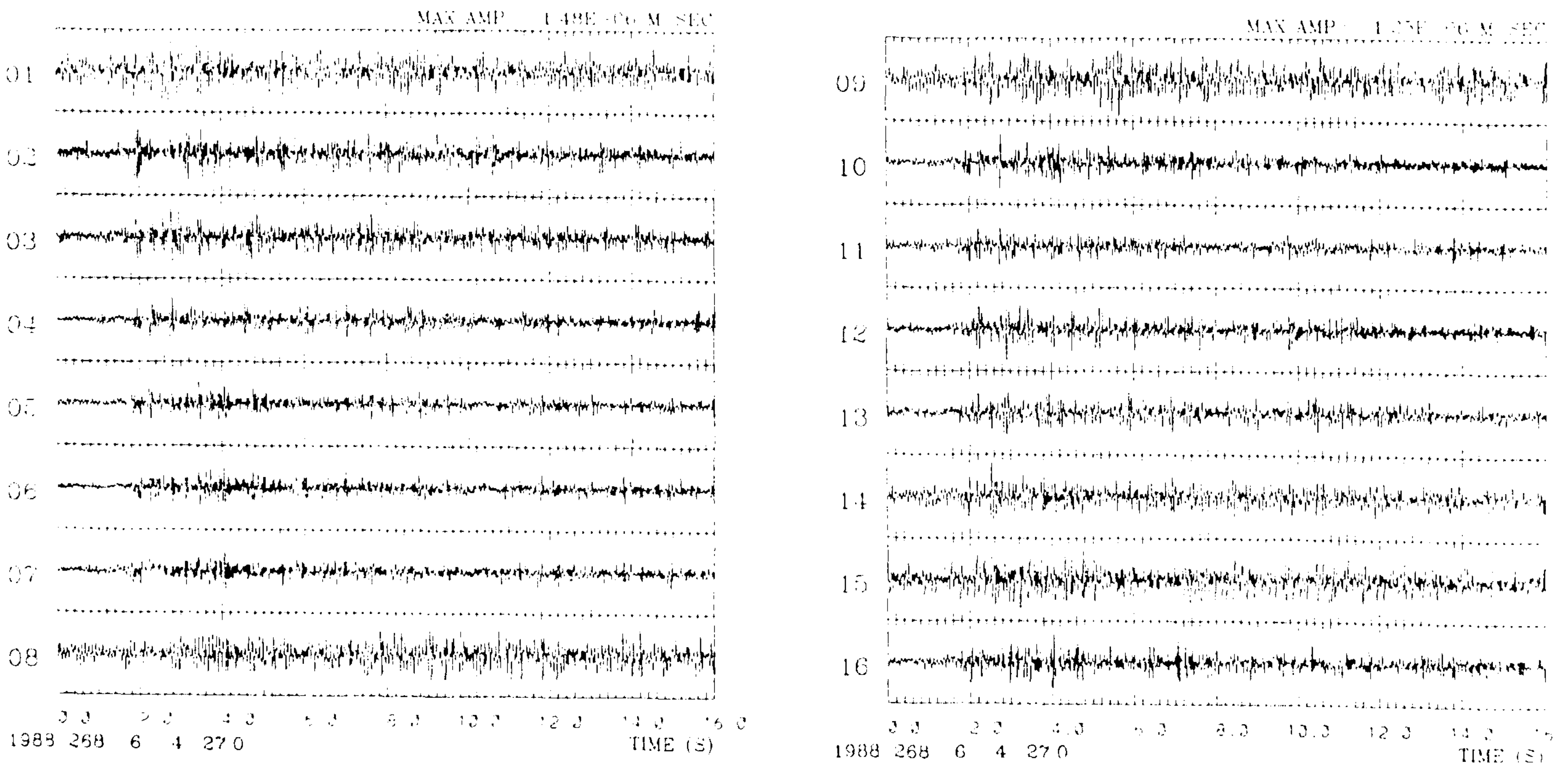

Figure 24. Instrument Response Corrected Traces for Channels 1 Through 8 (a) and 9 Through 16 (b) for Shot 13A as Recorded by the North Haverhill Array.

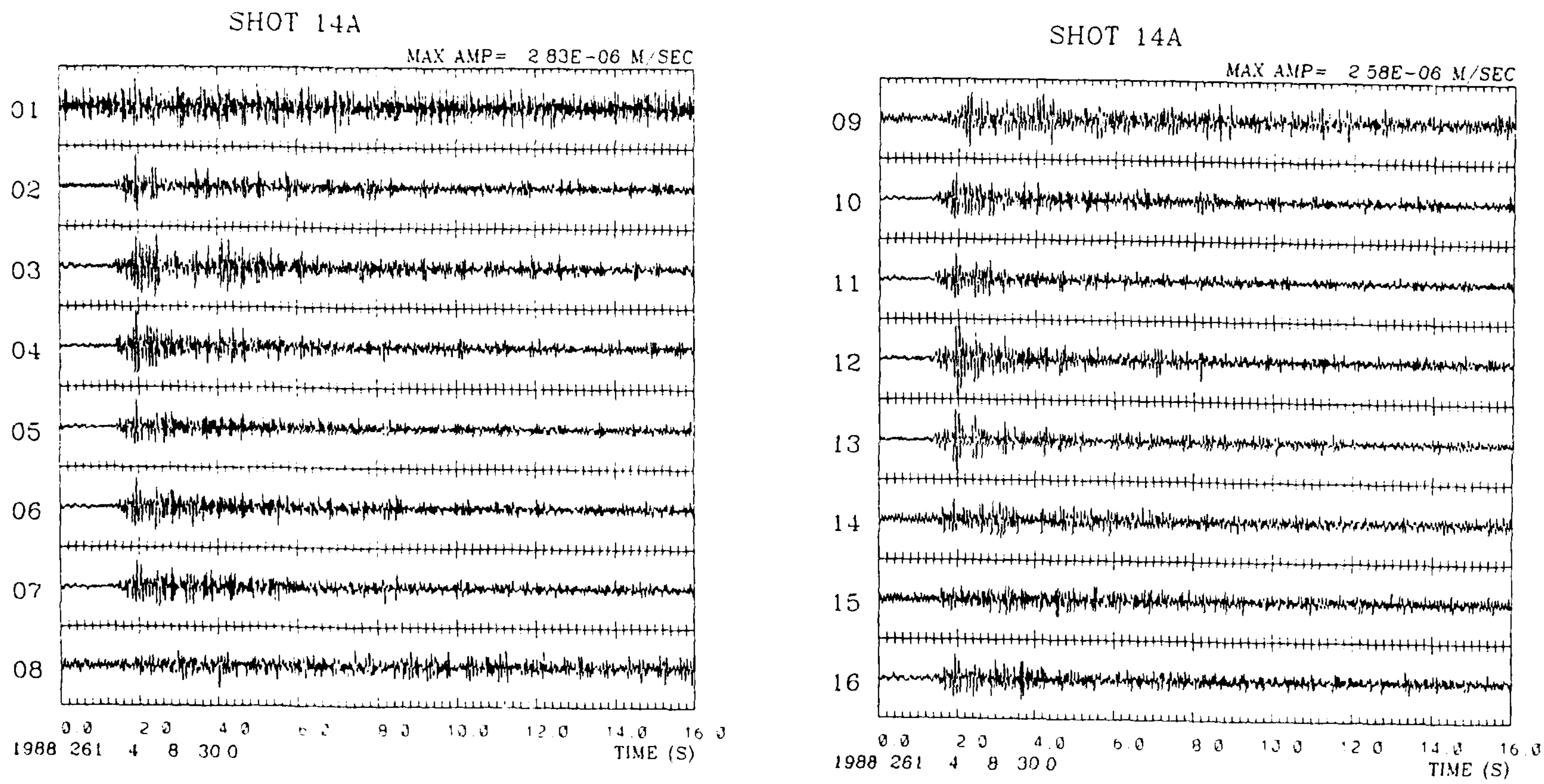

Figure 25. Instrument Response Corrected Traces for Channels 1 Through 8 (a) and 9 Through 16 (b) for Shot 14A as Recorded by the North Haverhill Array.

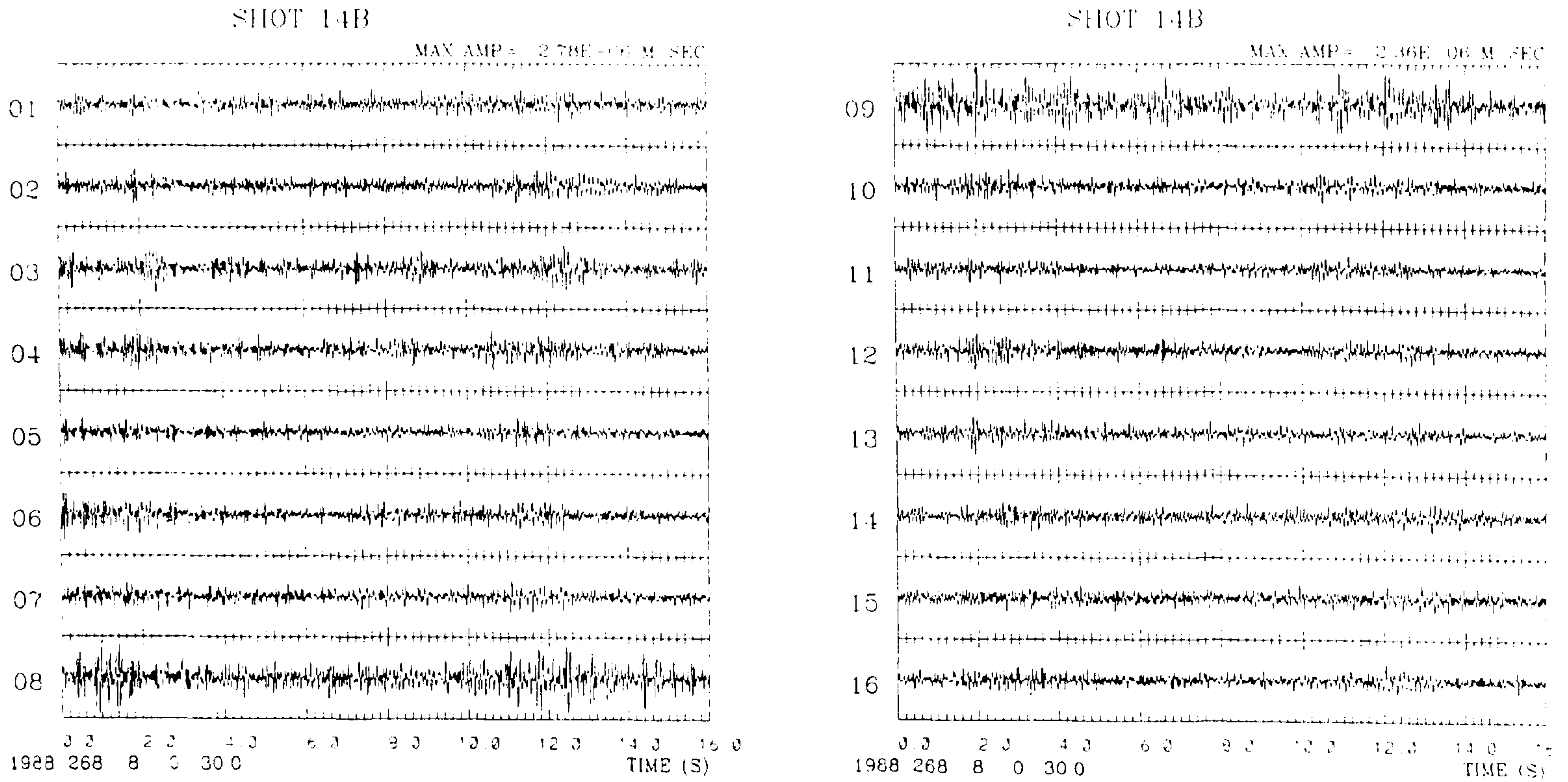

Figure 26. Instrument Response Corrected Traces for Channels 1 Through 8 (a) and 9 Through 16 (b) for Shot 14B as Recorded by the North Haverhill Array.

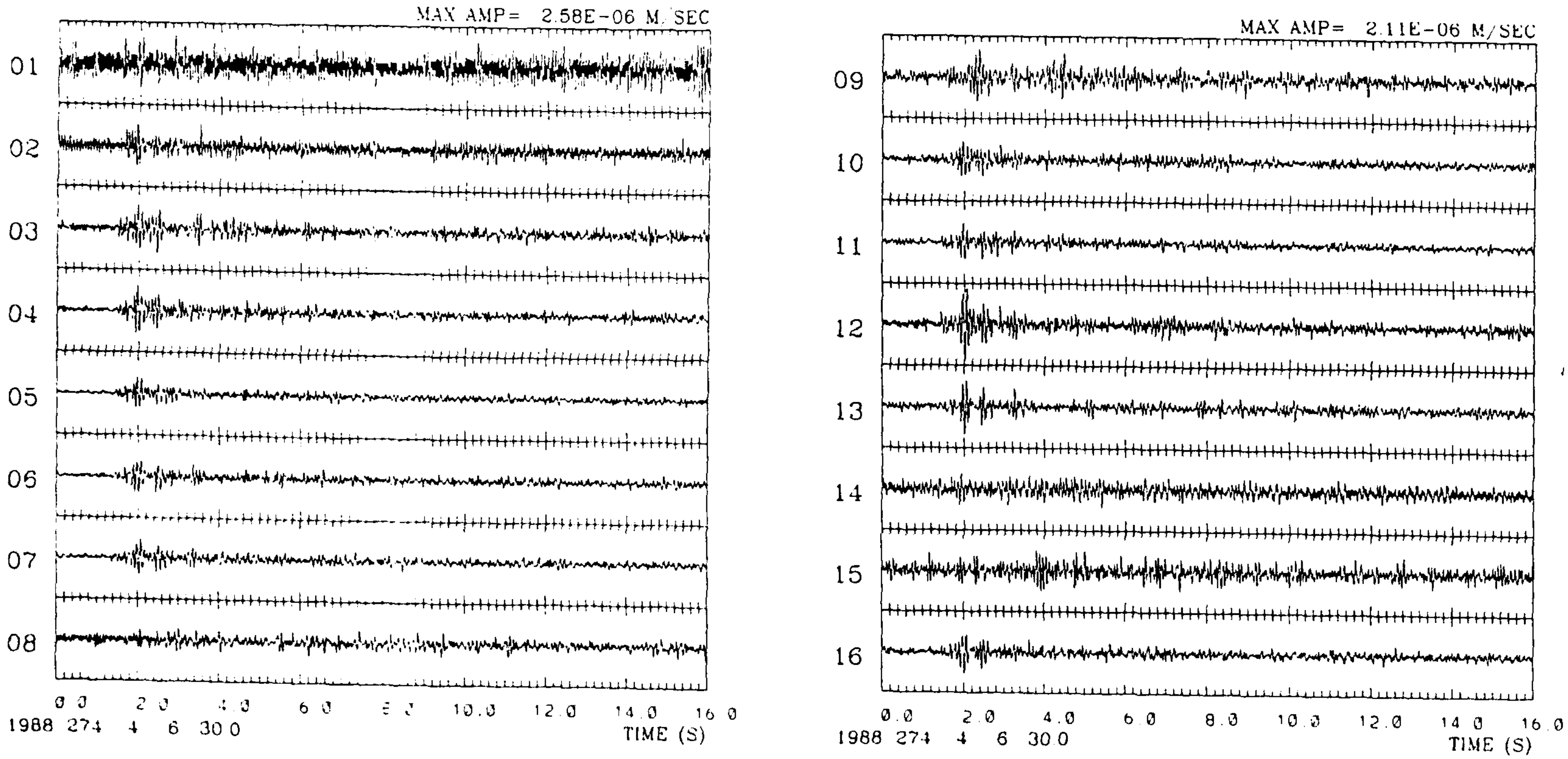

Figure 27. Instrument Response Corrected Traces for Channels 1 Through 8 (a) and 9 Through 16 (b) for Shot 14C as Recorded by the North Haverhill Array.

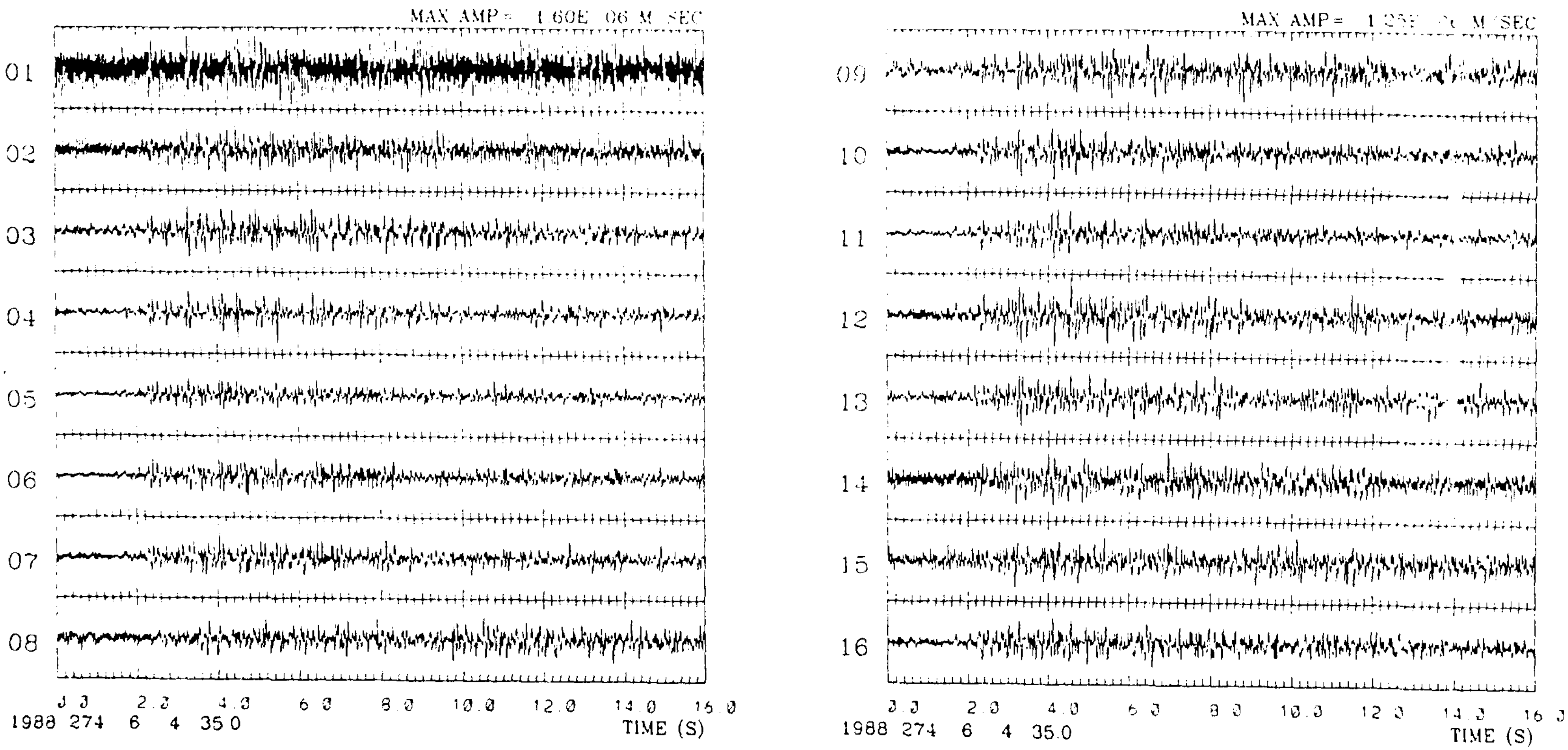

Figure 28. Instrument Response Corrected Traces for Channels 1 Through 8 (a) and 9 Through 16 (b) for Shot 15A as Recorded by the North Haverhill Array.

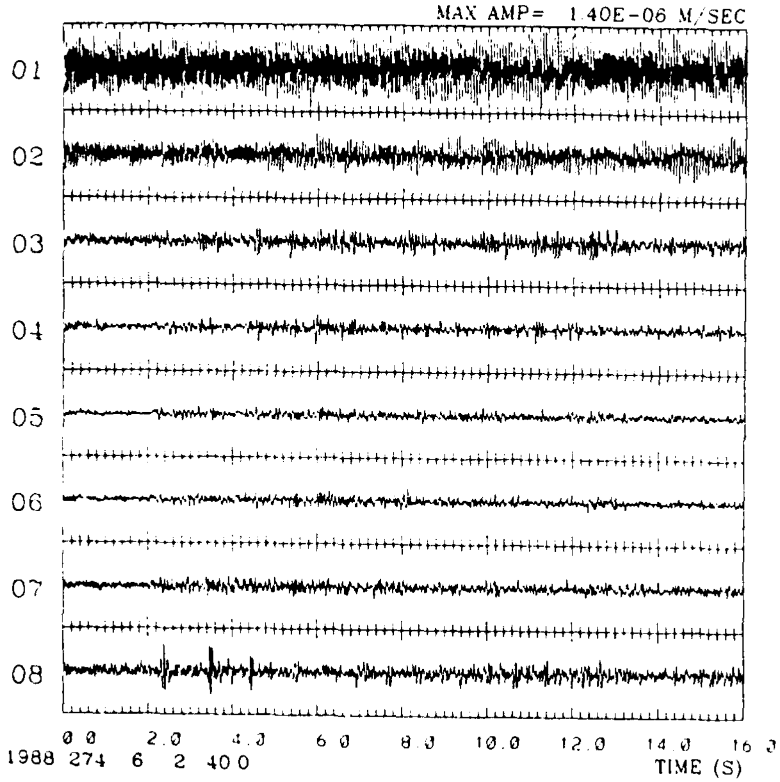

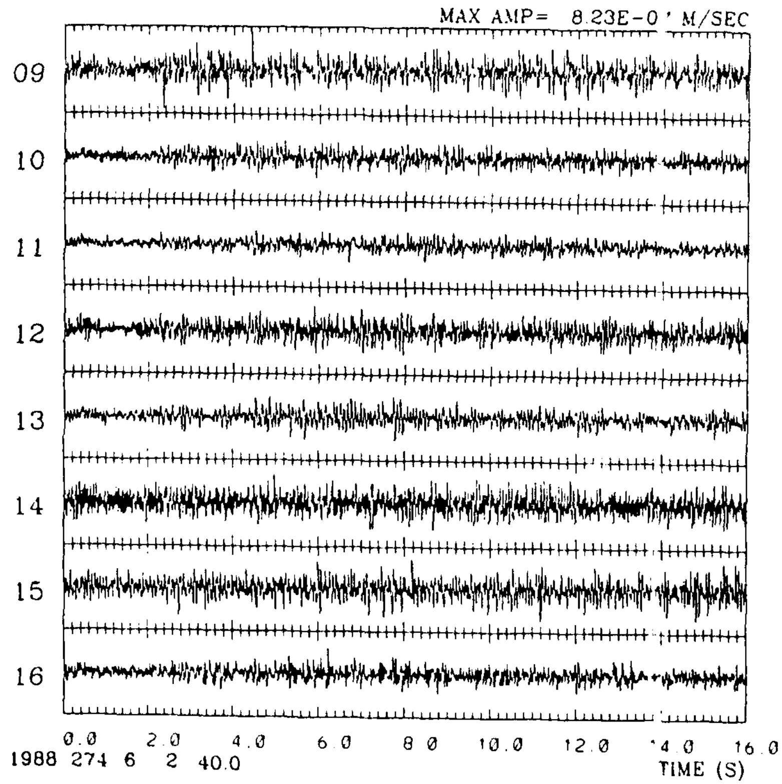

Figure 29. Instrument Response Corrected Traces for Channels 1 Through 8 (a) and 9 Through 16 (b) for Shot 16A as Recorded by the North Haverhill Array.

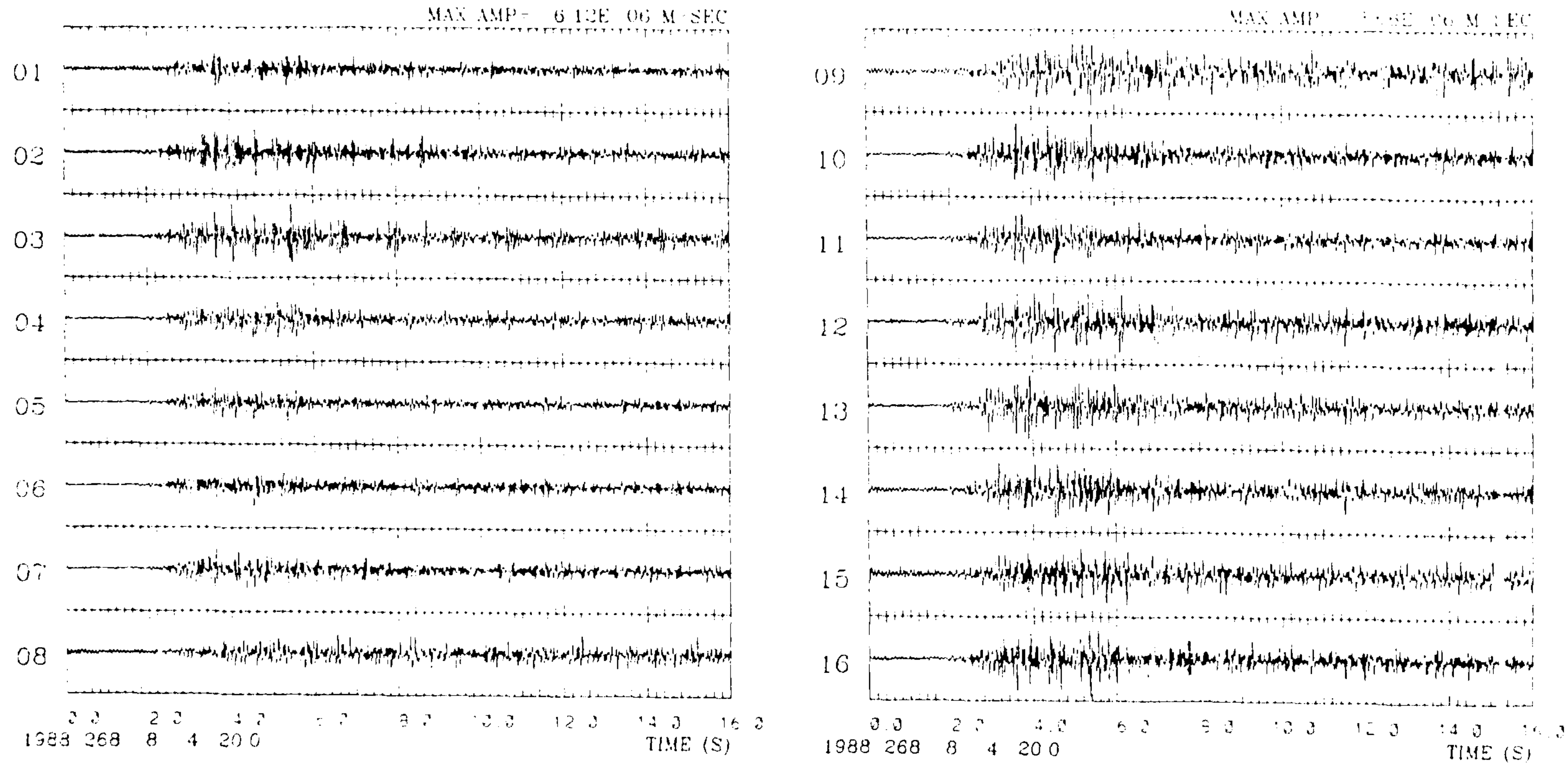

Figure 30. Instrument Response Corrected Traces for Channels 1 Through 8 (a) and 9 Through 16 (b) for Shot 21A as Recorded by the North Haverhill Array.

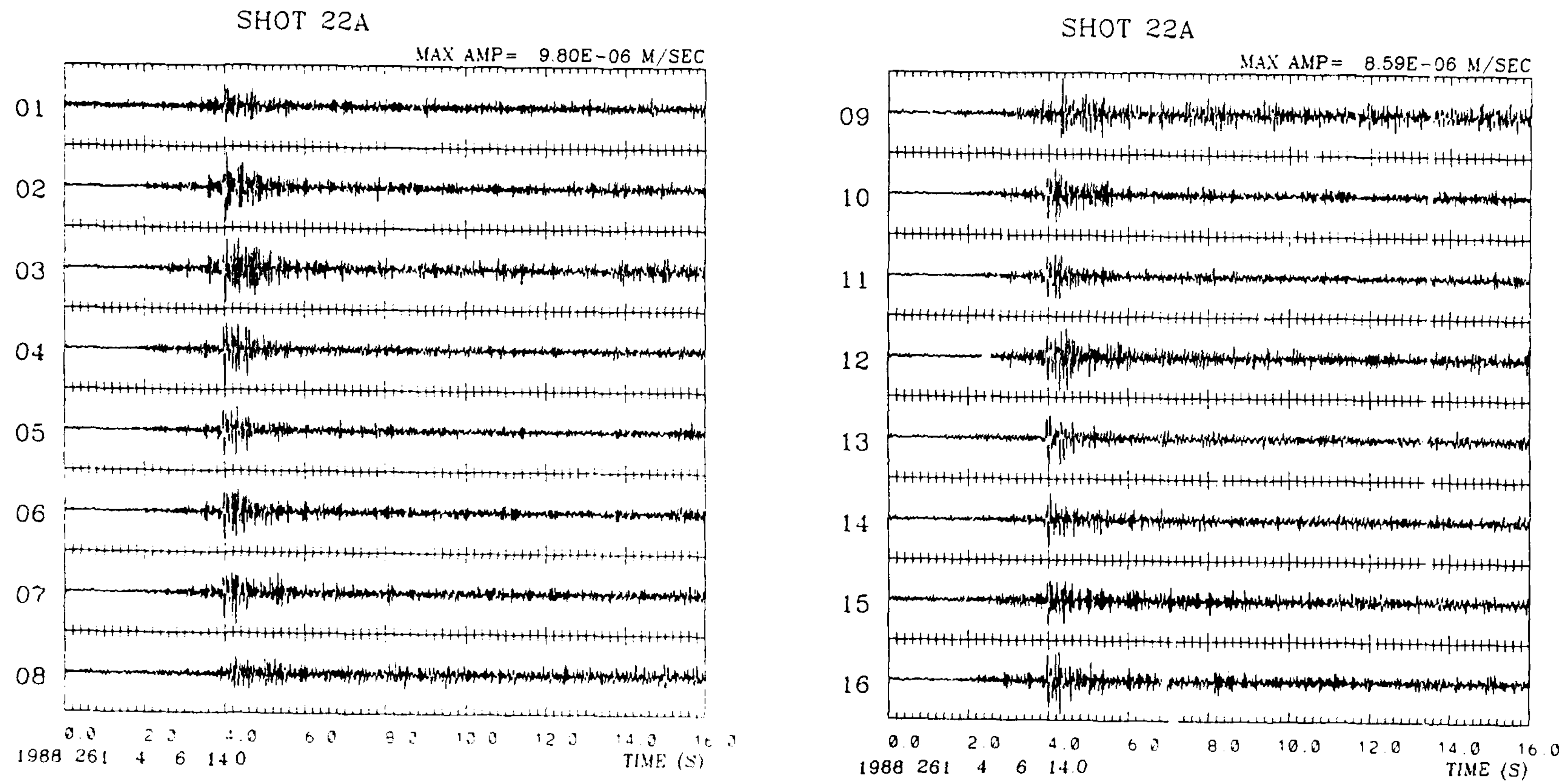

Figure 31. Instrument Response Corrected Traces for Channels 1 Through 8 (a) and 9 Through 16 (b) for Shot 22A as Recorded by the North Haverhill Array.

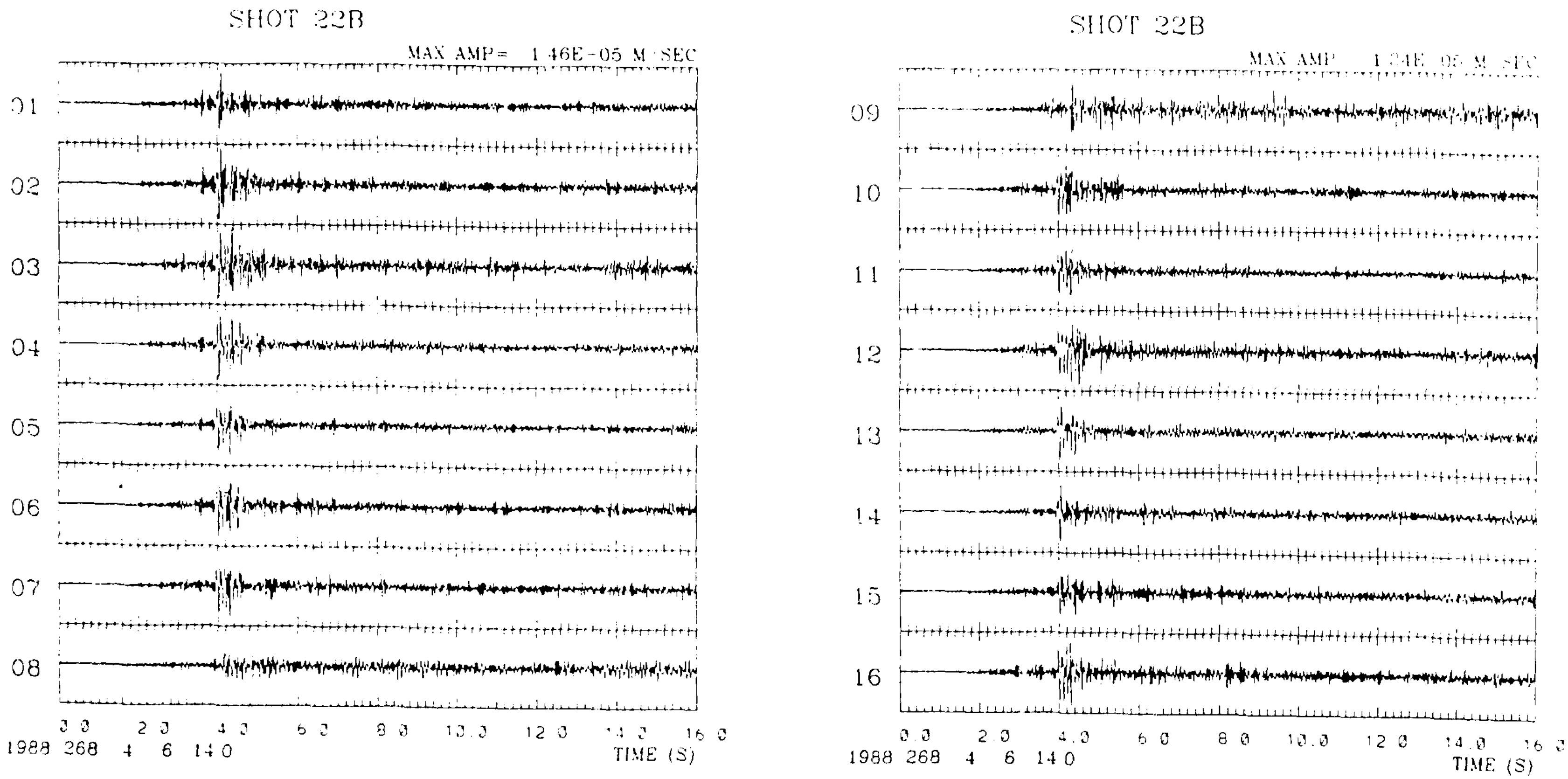

Figure 32. Instrument Response Corrected Traces for Channels 1 Through 8 (a) and 9 Through 16 (b) for Shot 22B as Recorded by the North Haverhill Array.

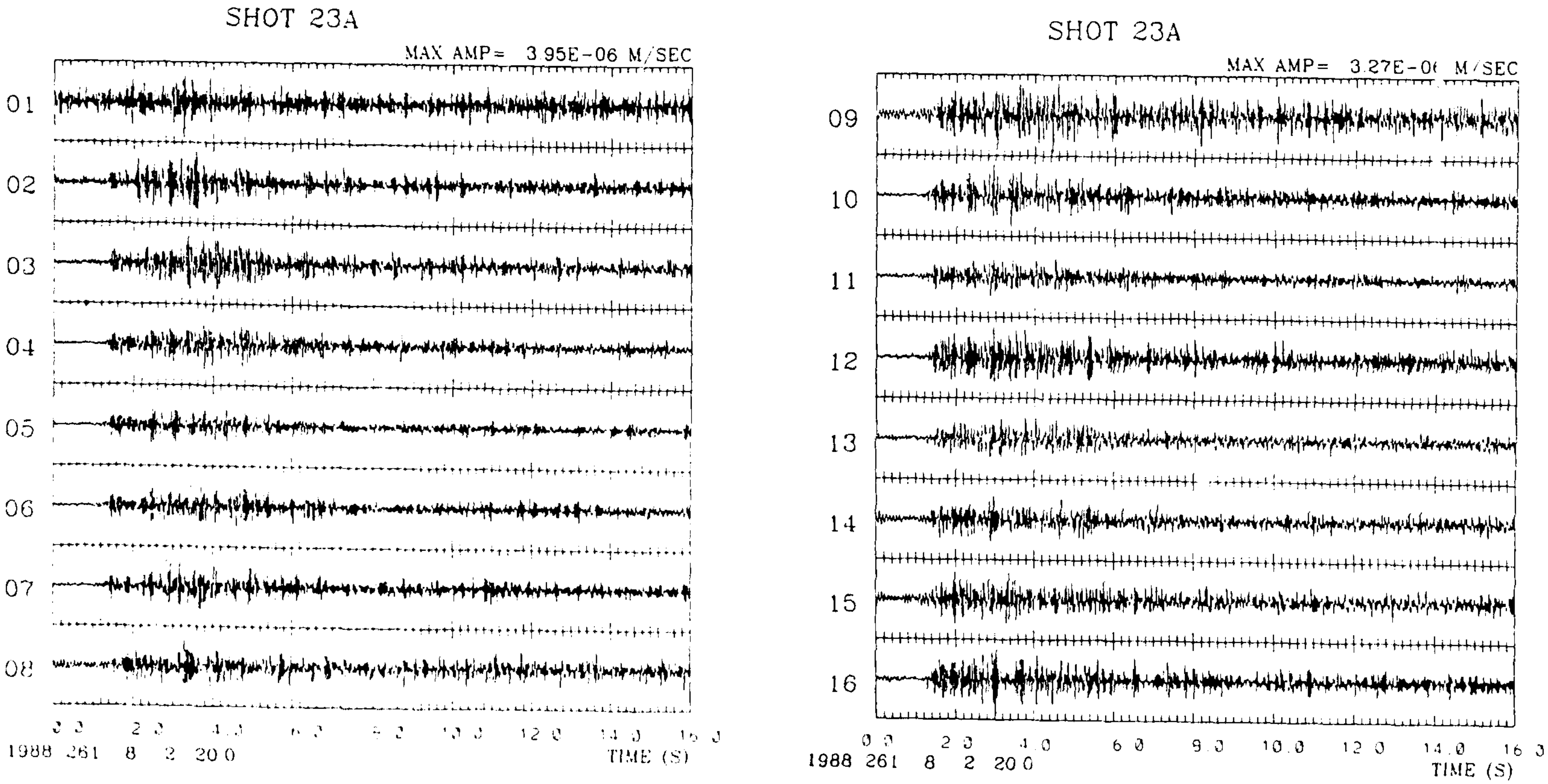

Figure 33. Instrument Response Corrected Traces for Channels 1 Through 8 (a) and 9 Through 16 (b) for Shot 23A as Recorded by the North Haverhill Array.

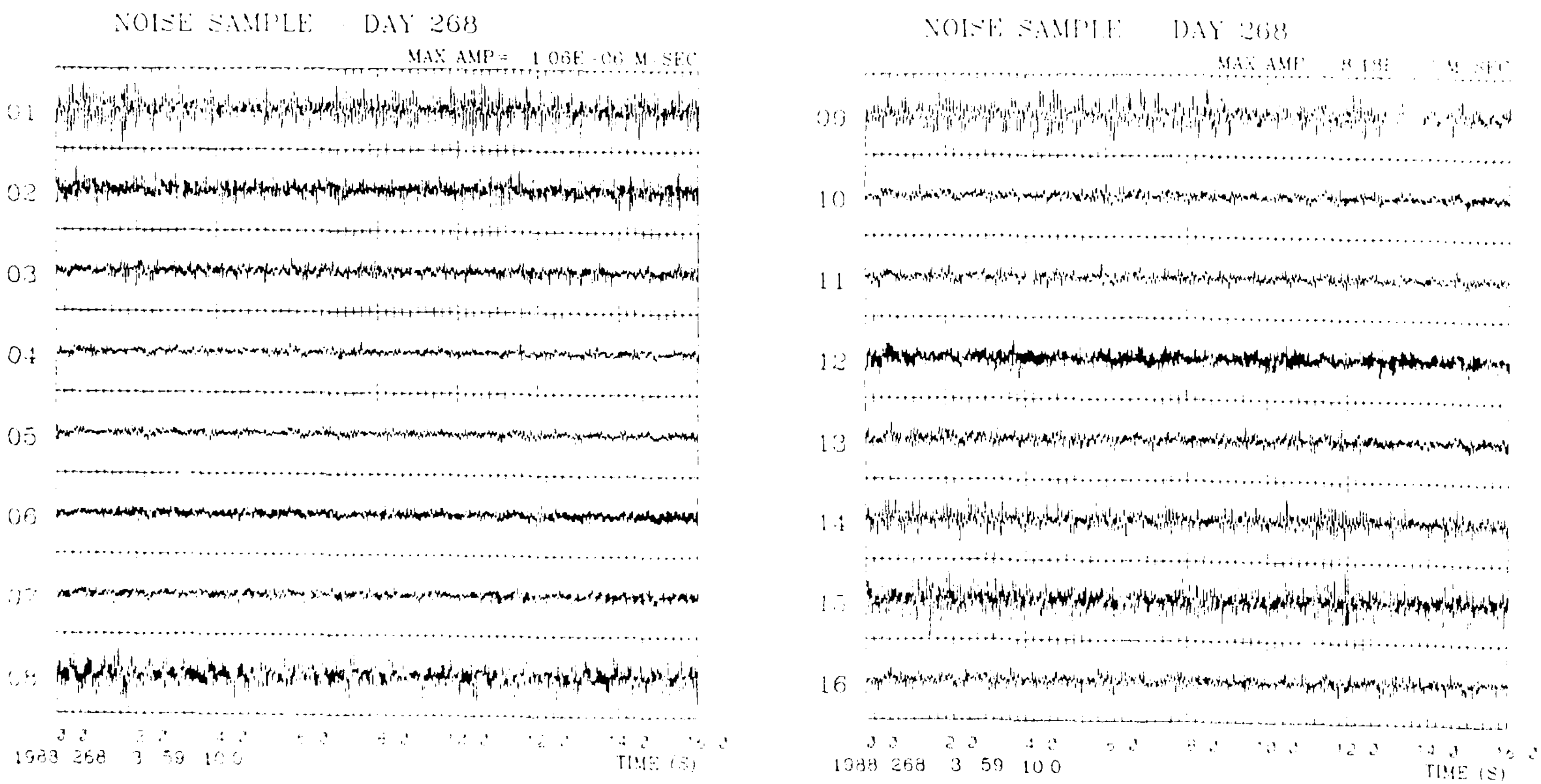

Figure 34. Typical Ambient Noise Sample for the North Haverhill Array Channels 1 Through 8 (a) and 9 Through 16 (b). In this case, the data was recorded just prior to the first shot window on 24 September.

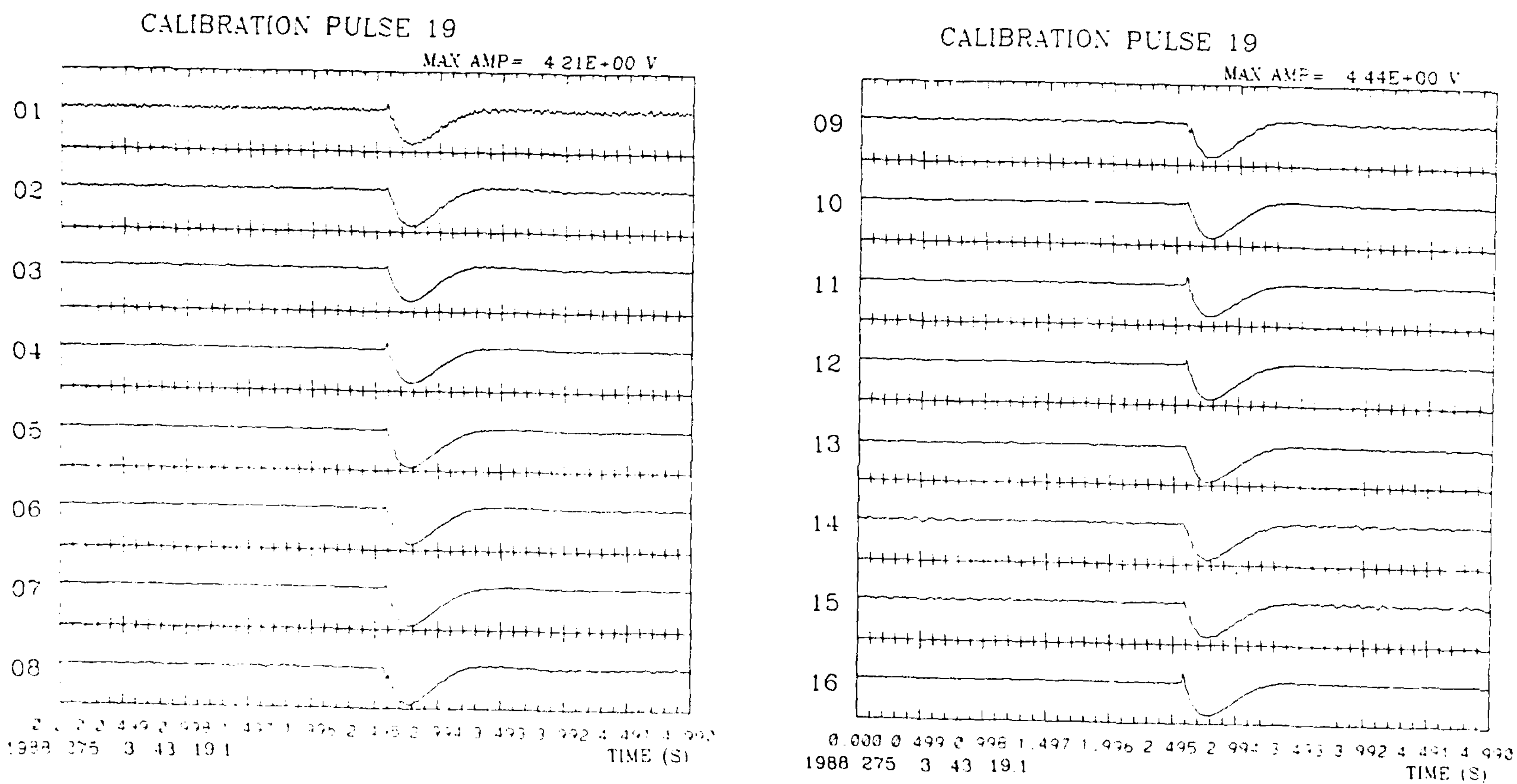

Figure 35. Typical Array Output Signals for an Input Calibration Pulse for the System in High Gain Configuration for Channels 1 Through 8 (a) and 9 Through 16 (b).

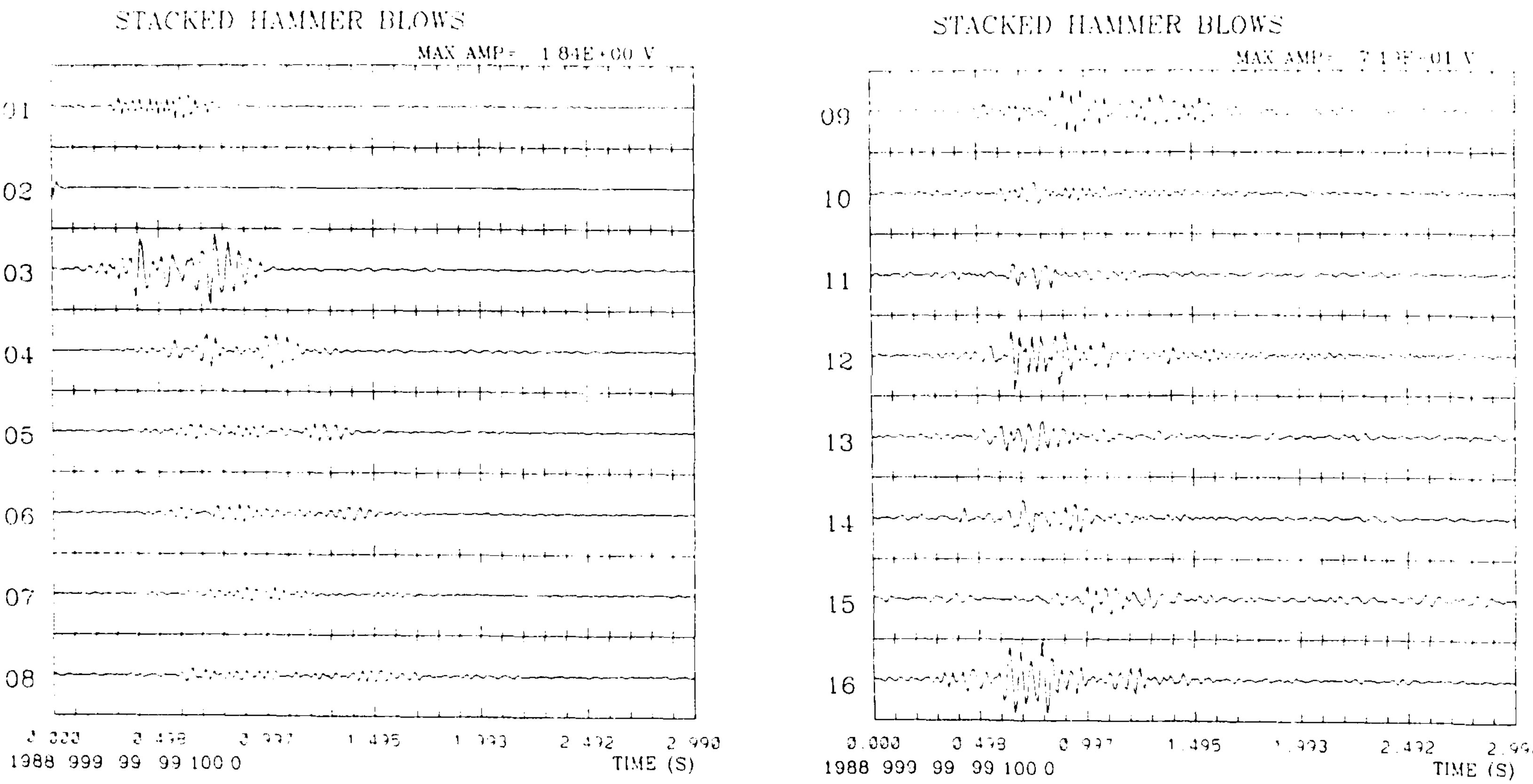

Figure 36. Typical Stacked Hammer Blow Data for Channels 1 Through 8 (a) and 9 Through 16 (b) with the Hammer at Sensor 2. A highpass filter with corner at 10.0 Hz has been applied to the data.

References

Blaney, J. (in preparation) *GDAS Hardware System Definition*, Boston College, Boston, MA.

Dewey, J.F. (1977) Suture Zone Complexities: A review, *Tectonophysics*, *v40*, pp53-67.

______ (1989) *Computer Programs in Seismology: PC Programs*, R.B. Hermann, ed., Saint Louis University, St. Louis, MO.

Moench, R.H. (1989) Metamorphic stratigraphy and structure of the Connecticut Valley area, Littleton to Piermont, New Hampshire in *A Transect Through the New England Appalachians*, J.B. Lyons and W.A. Bothner, ed., American Geophysical Union, Field Trip Guidebook T162, Washington, D.C.

Mangino, S. and Cipar, J. (1990) *Data Report for the 1988 Ontario-New York-New England Seismic Refraction Experiment: Three-Component Profiles*, GL Report No. GL-TR-90-0039, Hanscom AFB, MA., ADA221898.

von Glahn, P.G. (1980) *The Air Force Geophysics Laboratory Standalone Data Acquisition System: A Functional Description*, AFGL Report No. AFGL-TR-80-0317,Hanscom AFB, MA, ADA100253.